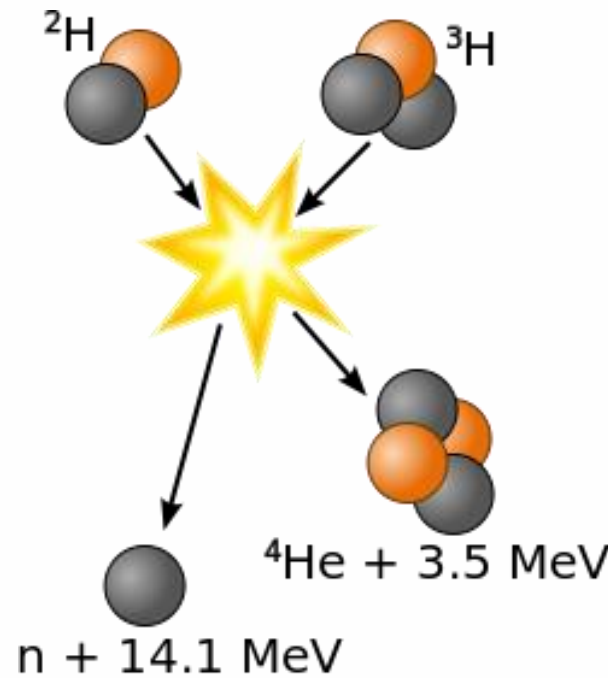


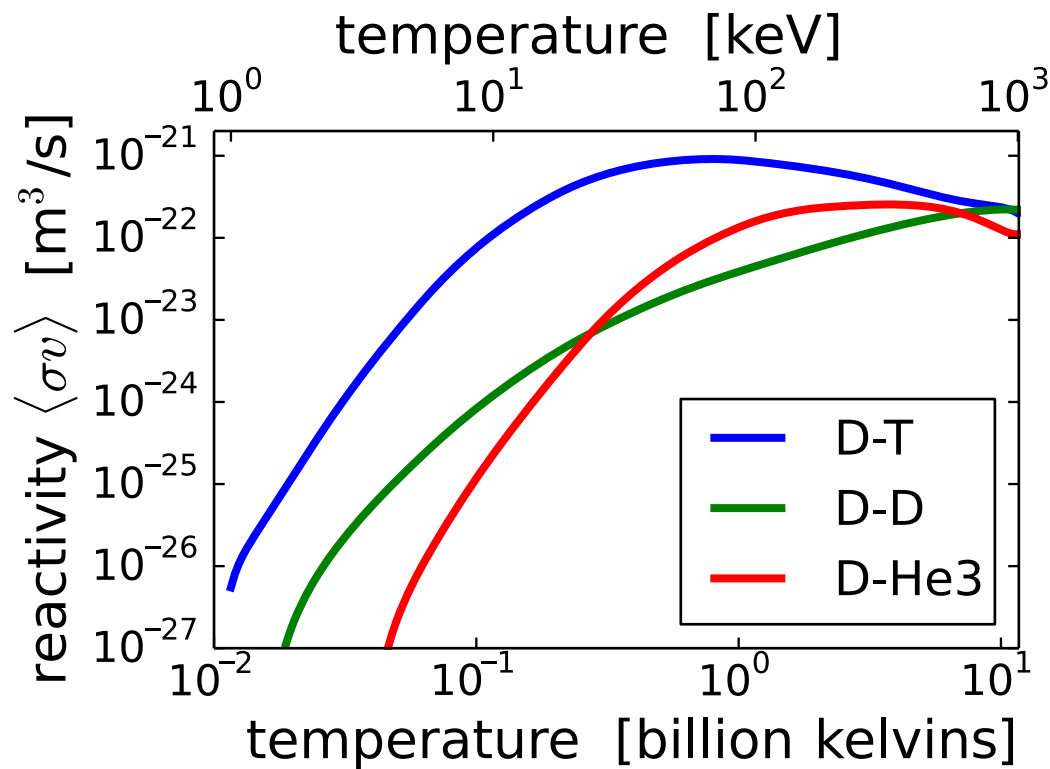
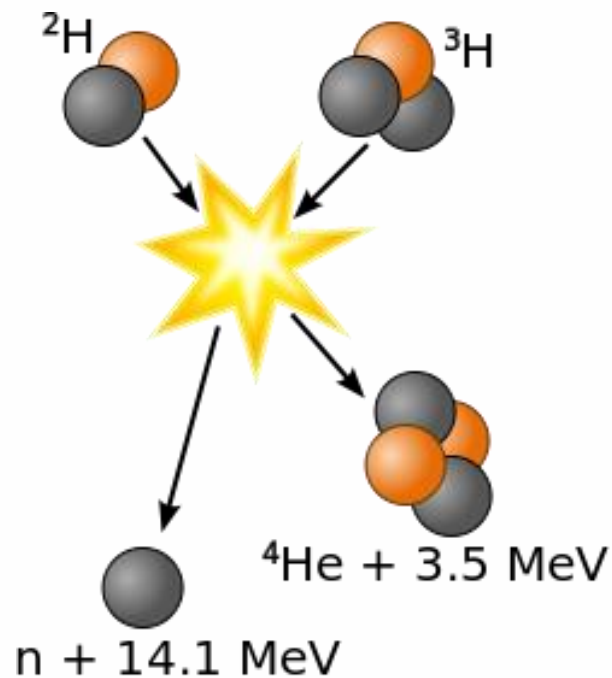
Runaway electrons in tungsten-rich tokamak plasmas

Jędrzej Walkowiak

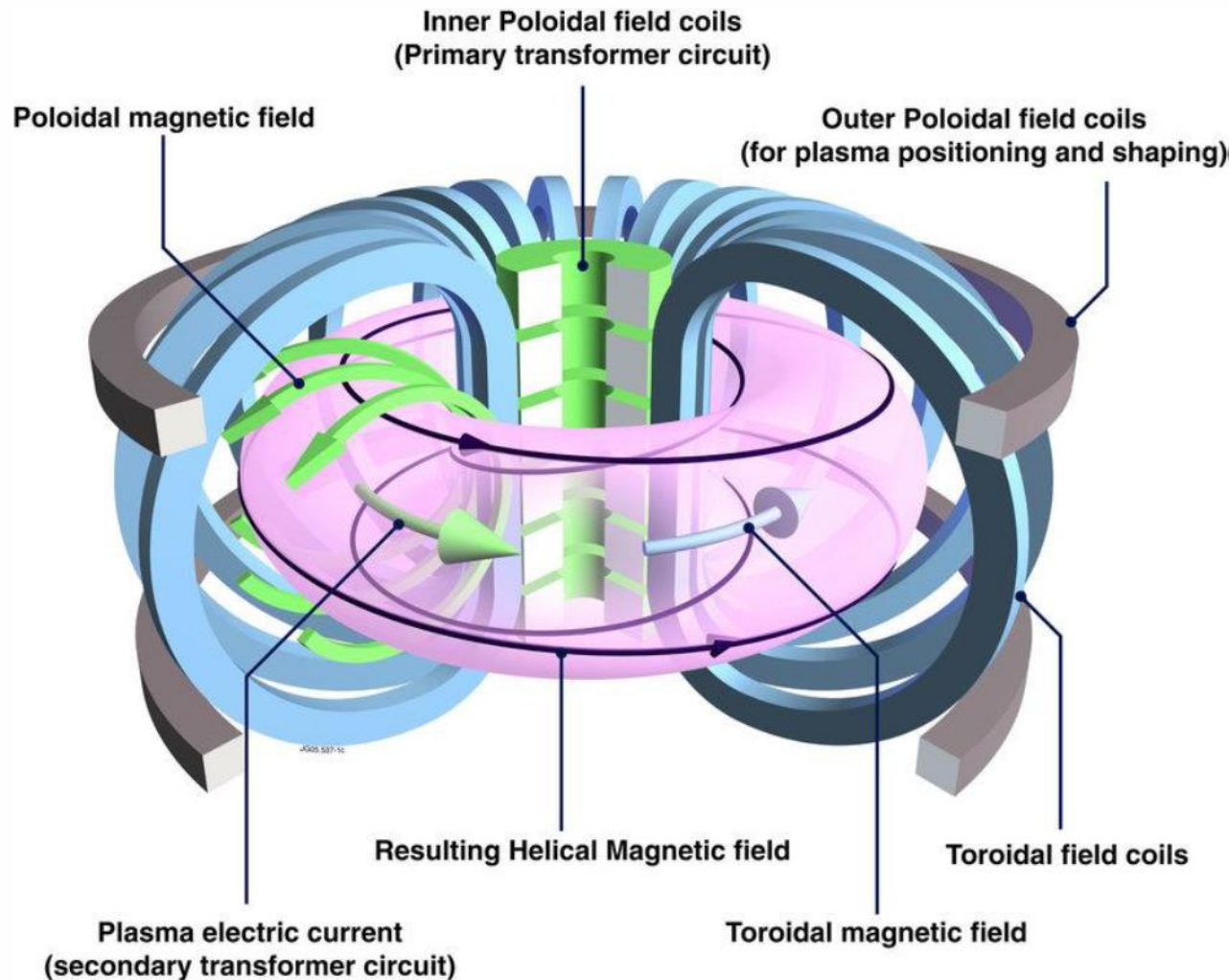
Zakład Fizyki Transportu Promieniowania (NZ61)

Kraków 22.02.2024

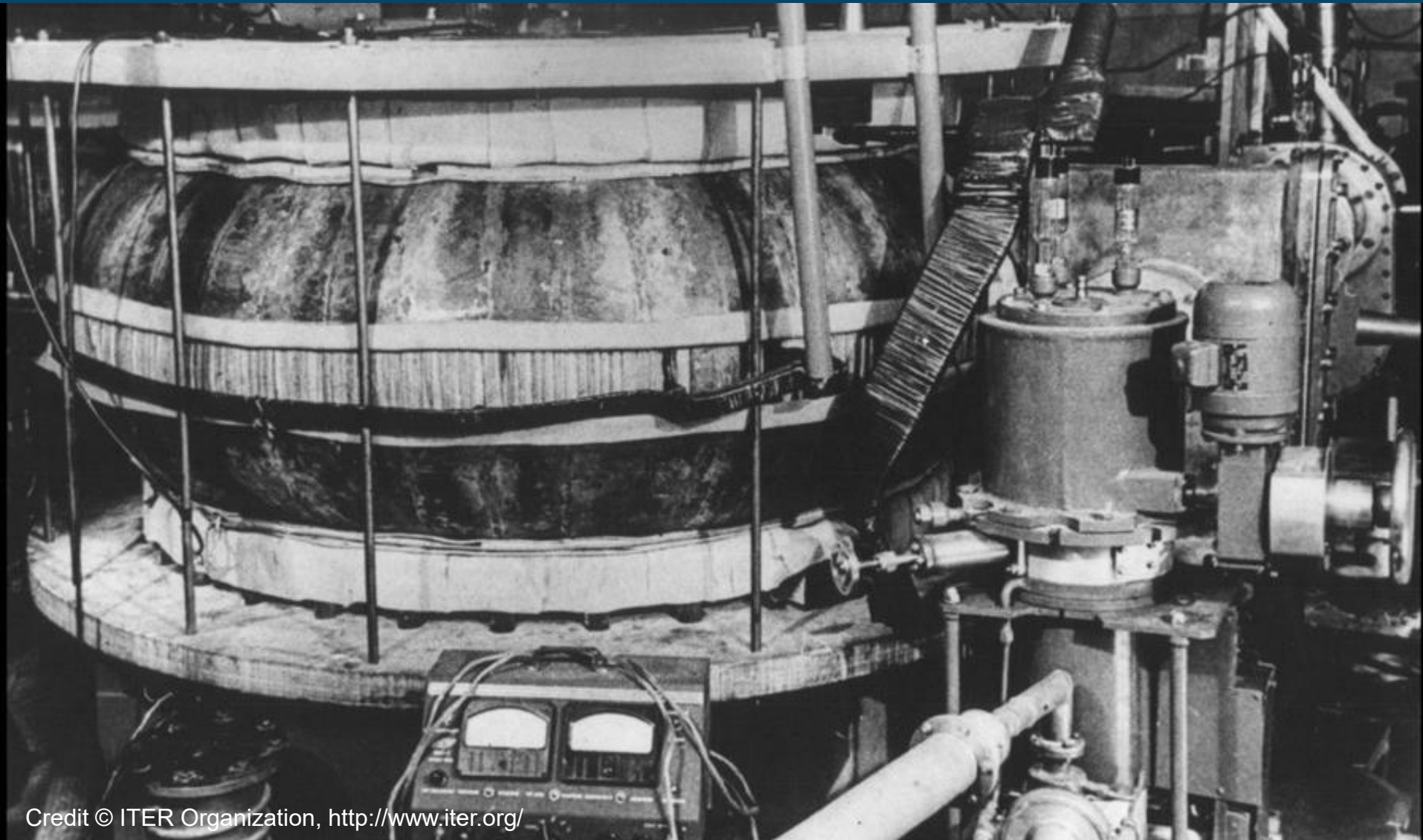




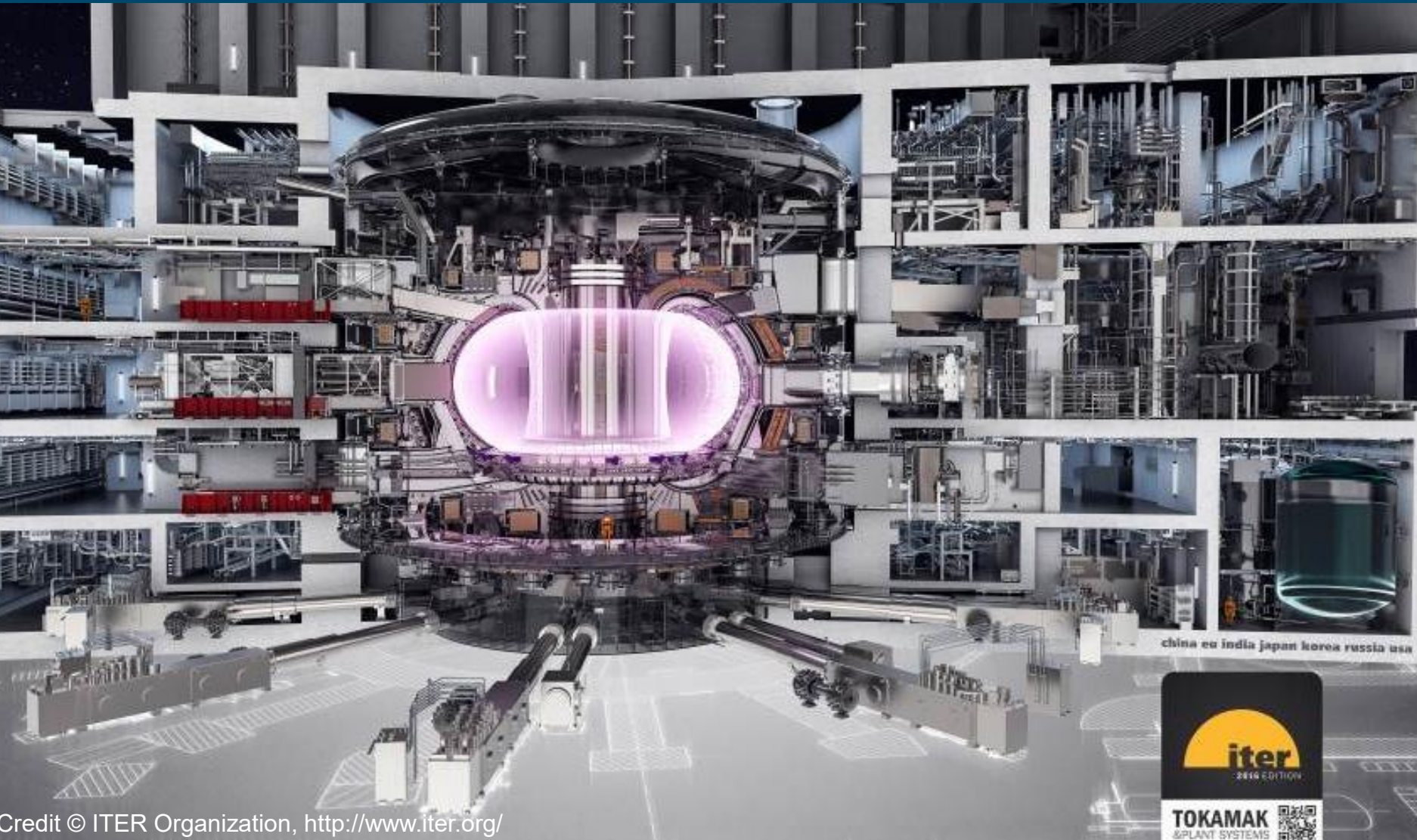
Credit © User: Dstrozzi / Wikimedia Commons / CC-BY-2.5



Source: S. Li et. al. *Abstract and Applied Analysis*, vol. 2014, Article ID 940965



Credit © ITER Organization, <http://www.iter.org/>



Credit © ITER Organization, <http://www.iter.org/>



THE HENRYK NIEWODNICZAŃSKI
INSTITUTE OF NUCLEAR PHYSICS
POLISH ACADEMY OF SCIENCES

Tokamak - ITER



Credit © ITER Organization, <http://www.iter.org/>

Time = 950.0 ms
Frame = 0



Fast electrons (non-Maxwellian)



Fast electrons (non-Maxwellian)

In plasma

With Tungsten impurities



Fast electrons (non-Maxwellian)

In plasma

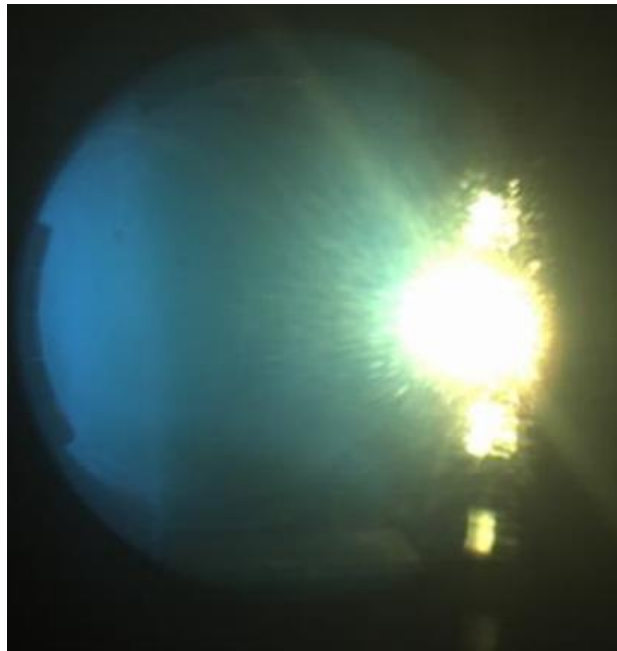
With Tungsten impurities

We want to predict their behaviour (dynamics)



Runaway electrons

Runaway electrons



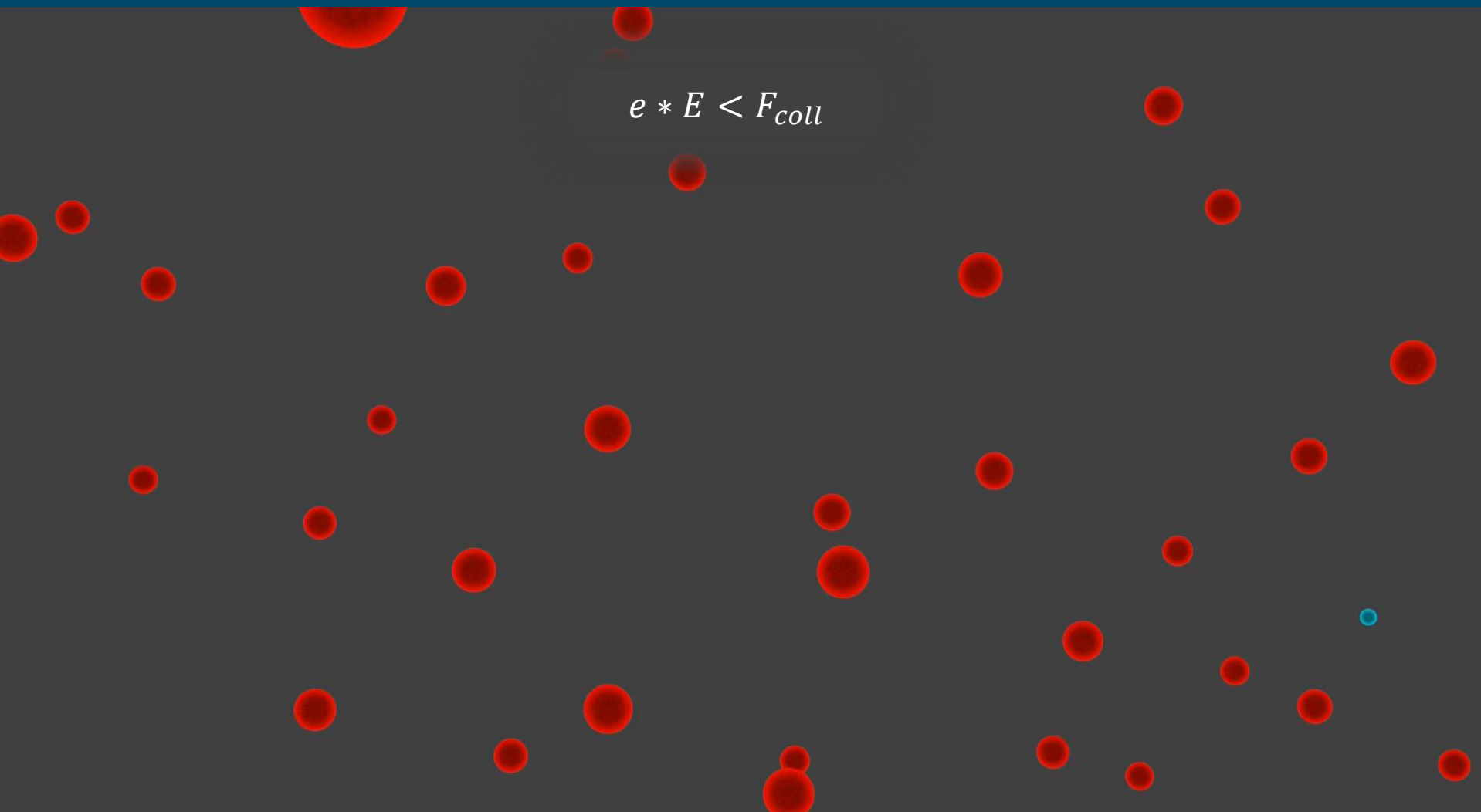
Source: V.P Budaev et al., Nucl. Mater. Energy. 12 (2017).
E. Joffrin et al, 5th REM meeting 2017.



$$-F = e * E$$

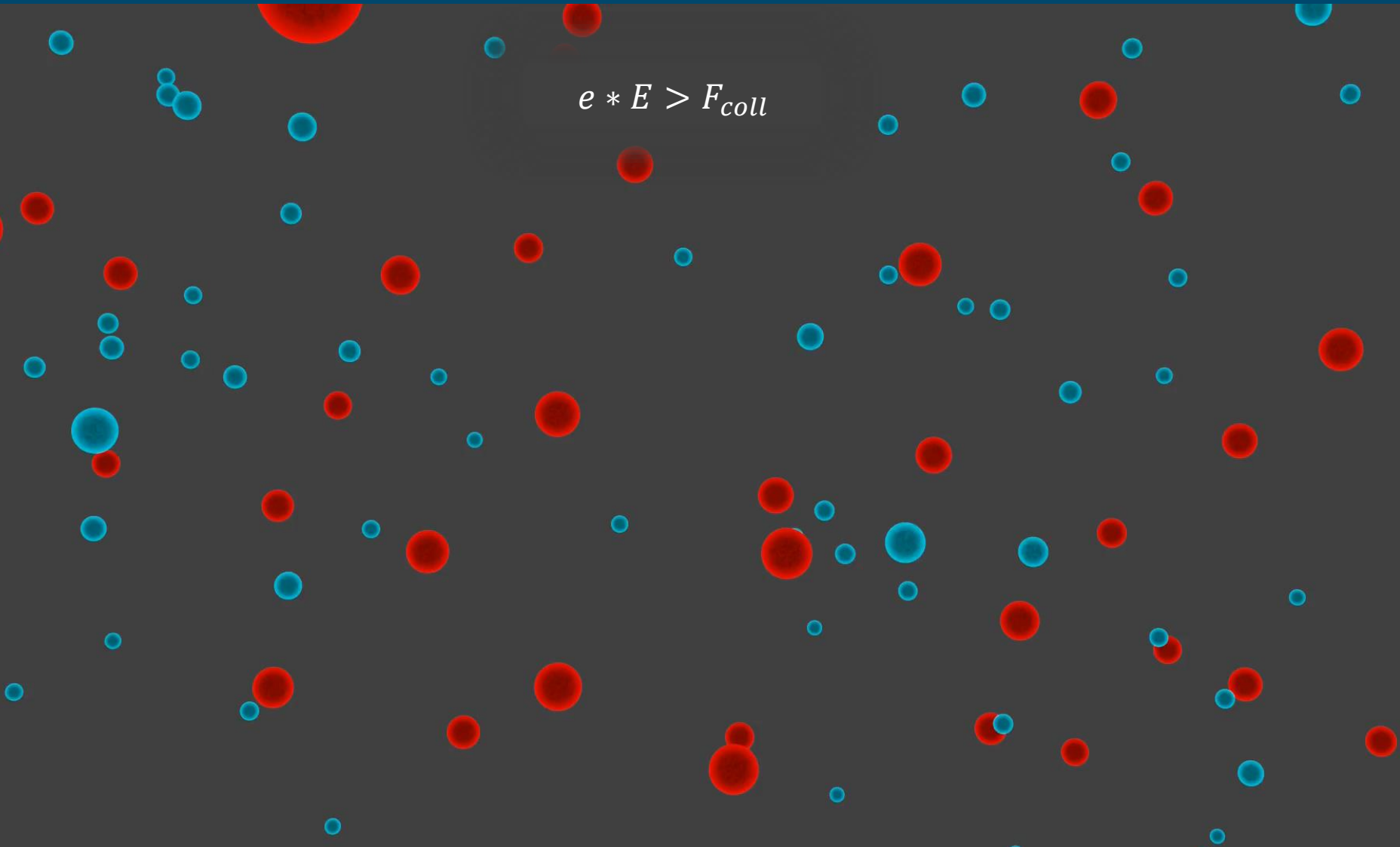
Runaway electrons

$$e * E < F_{coll}$$



Runaway electrons

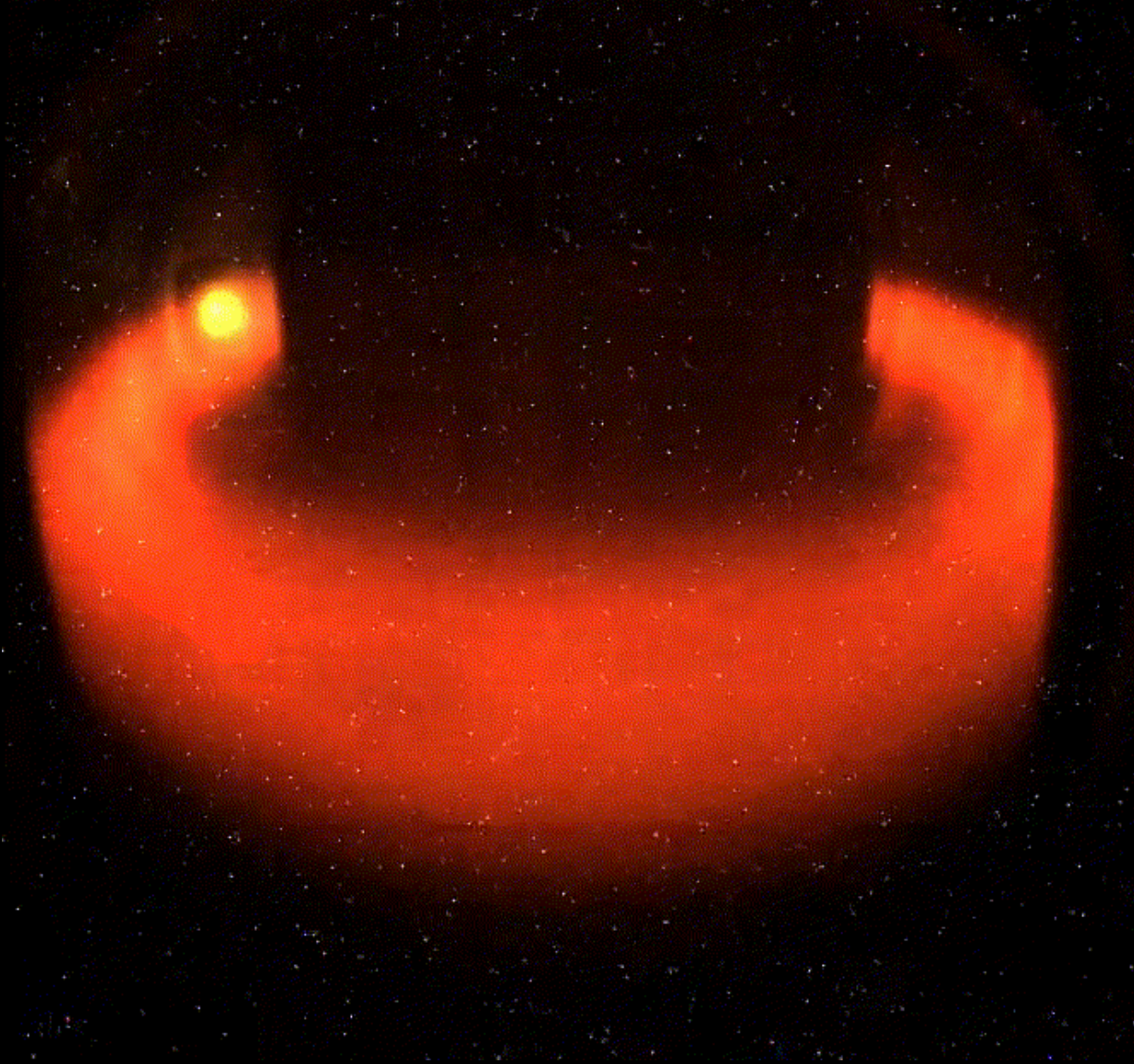
$$e * E > F_{coll}$$





Time = 1488.5 ms

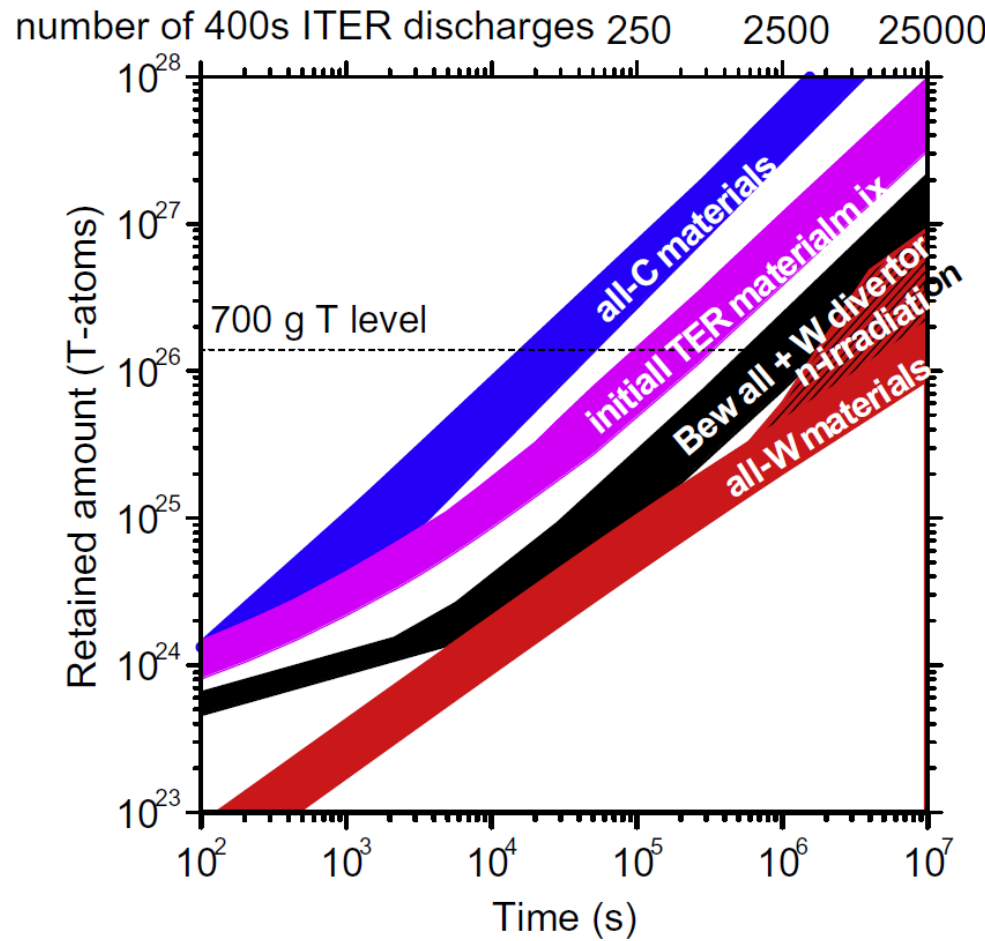
Frame = 2154



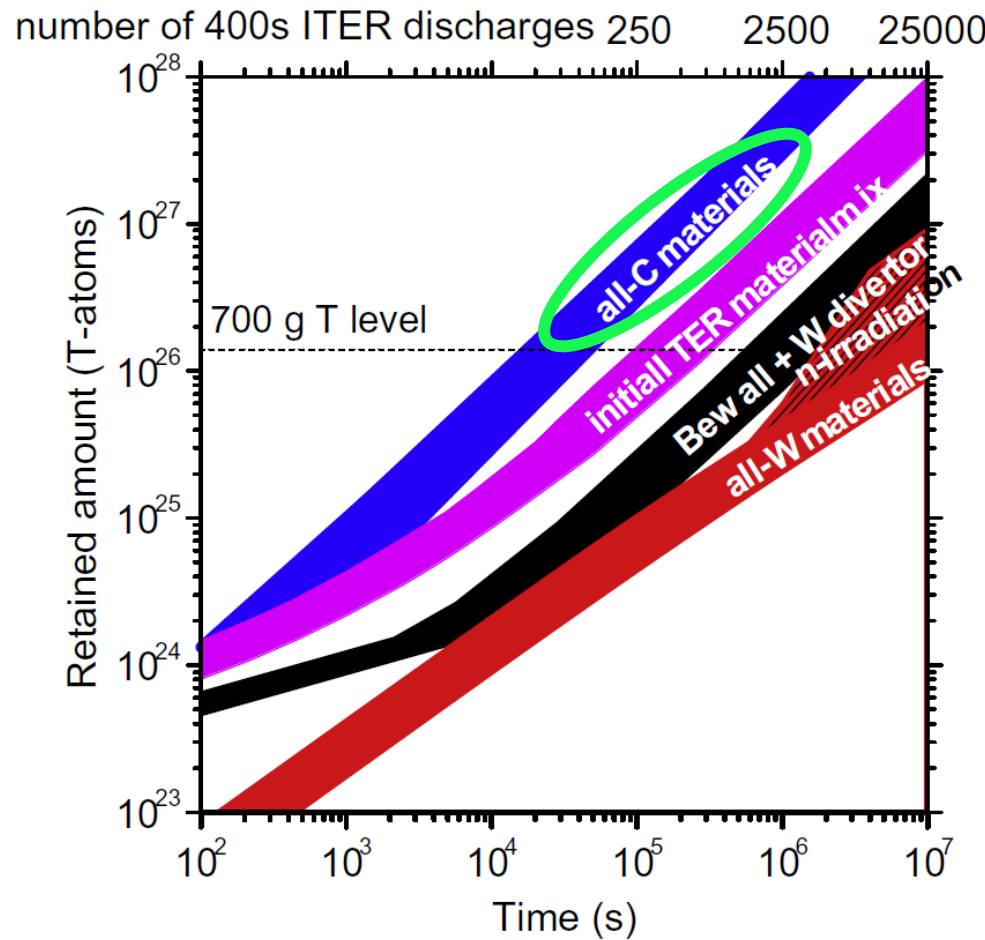
Runaway electrons in tungsten-rich tokamak
plasmas, J. Walkowiak



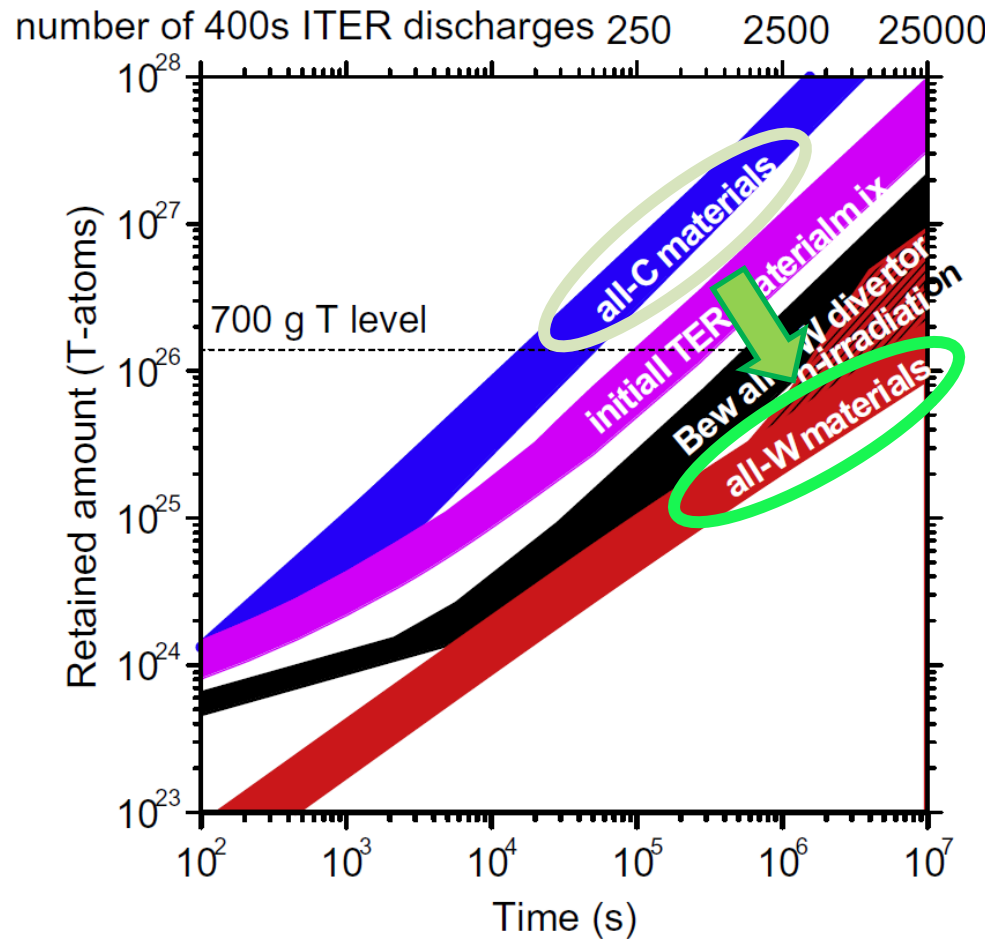
Tungsten impurities



Source: J Roth et al., J. Nucl. Mater. 390 (2009)

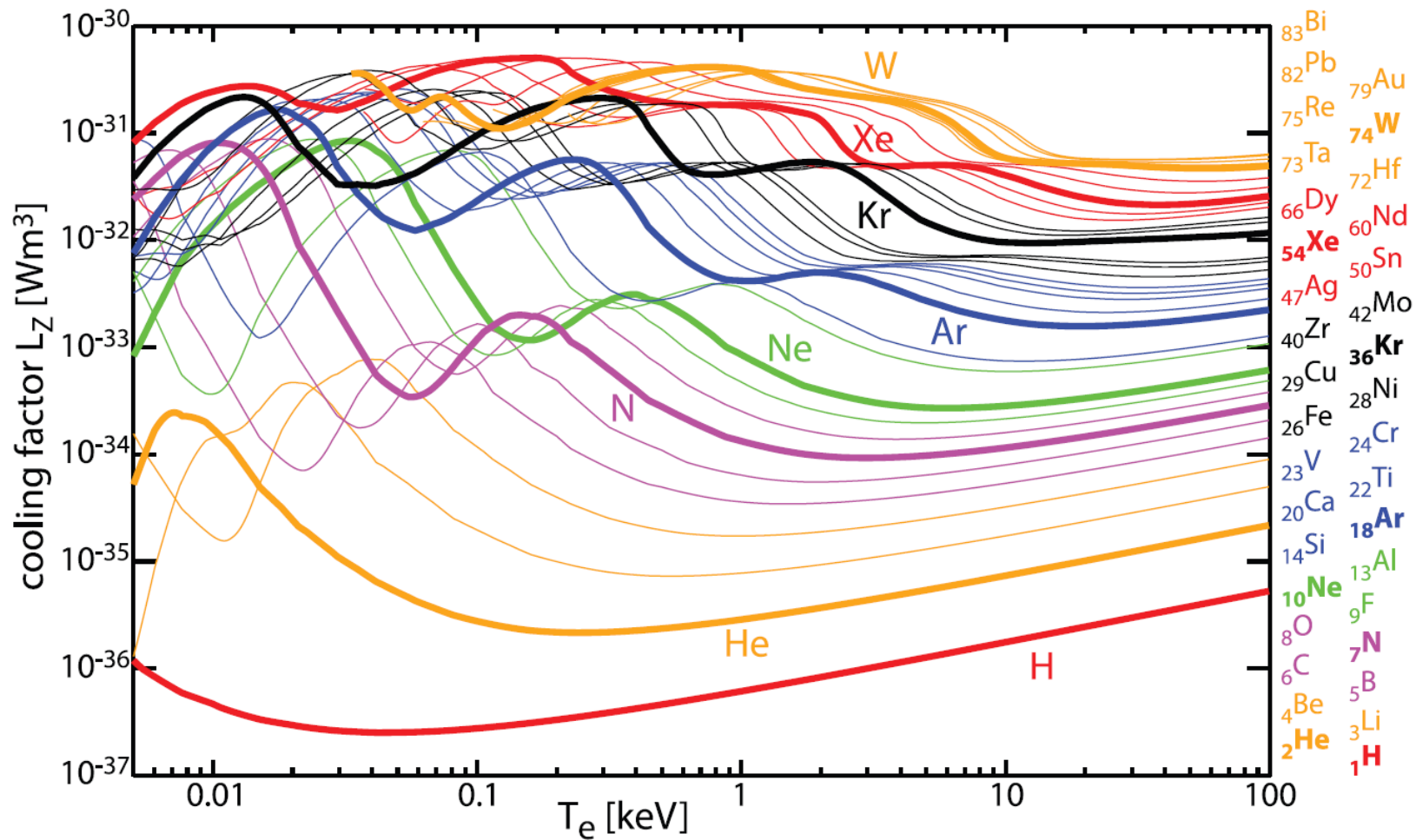


Source: J Roth et al., J. Nucl. Mater. 390 (2009)



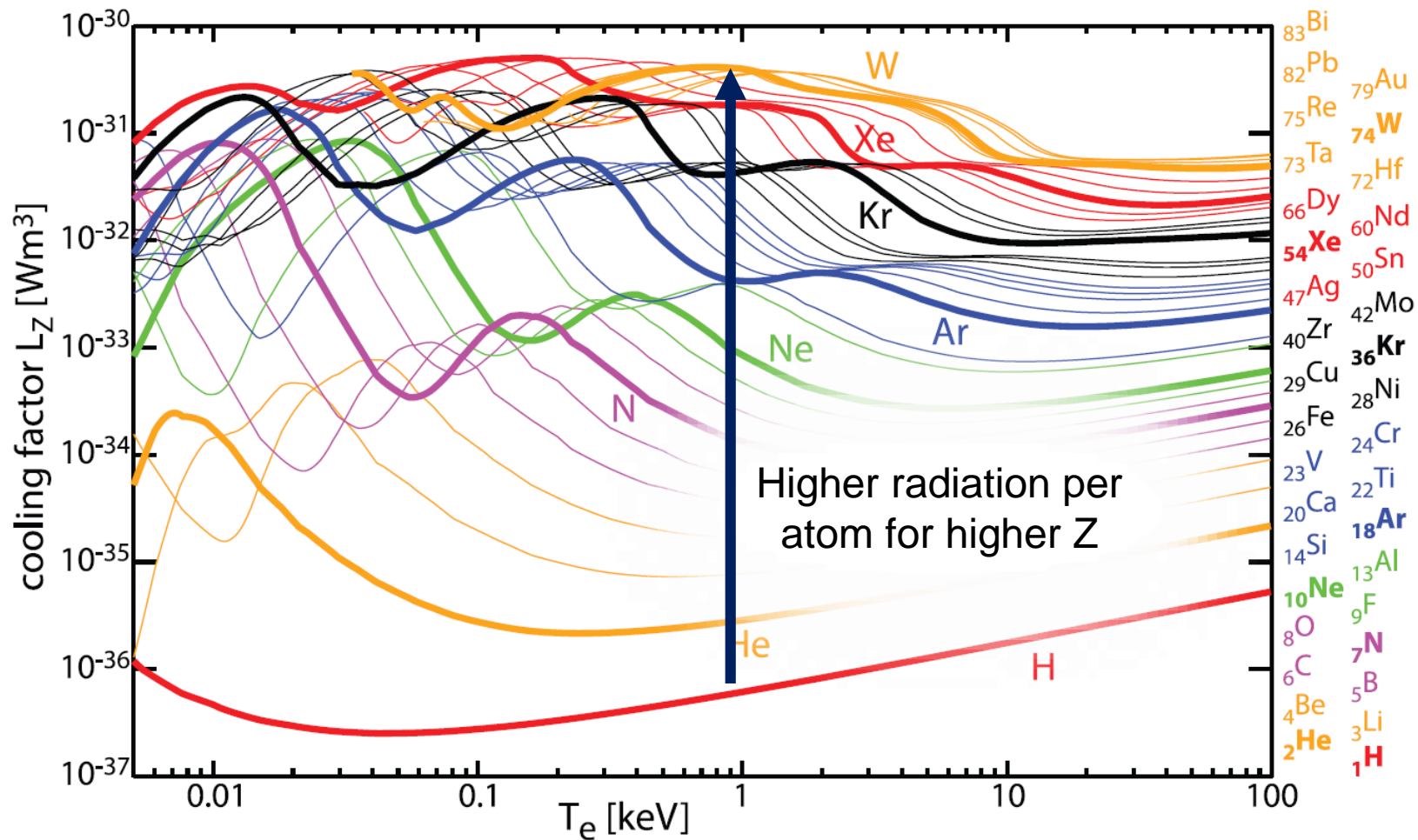
Source: J Roth et al., J. Nucl. Mater. 390 (2009)

Tungsten impurities



Source: T. Pütterich et al, Nucl. Fusion 59 056013 (2019)

Tungsten impurities



Source: T. Pütterich et al, Nucl. Fusion 59 056013 (2019)



Plasma modeling: Fokker-Planck equation

Fokker-Planck collision operator

$$C^{ab} = \nu_D^{ab} \mathcal{L}(f_a) + \frac{1}{p^2} \frac{\partial}{\partial p} \left[p^3 \nu_s^{ab} f_a + \frac{1}{2} \nu_{||}^{ab} \frac{\partial f_a}{\partial p} \right]$$

C^{ab} - collision operator for collisions between particle species a and b ,
 $\mathcal{L}(f_a)$ – Lorentz scattering operator,
 p – normalized momentum,
 f_a - velocity distribution function of species a .

Fokker-Planck collision operator

$$C^{ab} = \nu_D^{ab} \mathcal{L}(f_a) + \frac{1}{p^2} \frac{\partial}{\partial p} \left[p^3 \nu_s^{ab} f_a + \frac{1}{2} \nu_{||}^{ab} \frac{\partial f_a}{\partial p} \right]$$

C^{ab} - collision operator for collisions between particle species a and b ,
 $\mathcal{L}(f_a)$ – Lorentz scattering operator,
 p – normalized momentum,
 f_a - velocity distribution function of species a .

Fokker-Planck collision operator

$$C^{ab} = \nu_D^{ab} \mathcal{L}(f_a) + \frac{1}{p^2} \frac{\partial}{\partial p} \left[p^3 \nu_s^{ab} f_a + \frac{1}{2} \nu_{||}^{ab} \frac{\partial f_a}{\partial p} \right]$$


Deflection frequency
(elastic collisions)

C^{ab} - collision operator for collisions between particle species a and b ,
 $\mathcal{L}(f_a)$ – Lorentz scattering operator,
 p – normalized momentum,
 f_a - velocity distribution function of species a .

Fokker-Planck collision operator

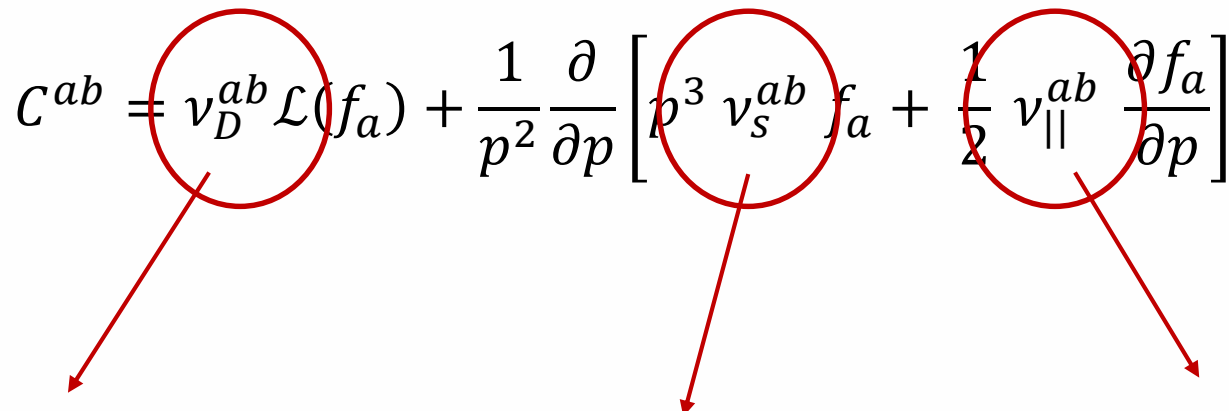
$$C^{ab} = \nu_D^{ab} \mathcal{L}(f_a) + \frac{1}{p^2} \frac{\partial}{\partial p} \left[p^3 \nu_s^{ab} f_a + \frac{1}{2} \nu_{||}^{ab} \frac{\partial f_a}{\partial p} \right]$$

Deflection frequency
(elastic collisions)

Slowing-down
frequency
(inelastic collisions)

C^{ab} - collision operator for collisions between particle species a and b ,
 $\mathcal{L}(f_a)$ – Lorentz scattering operator,
 p – normalized momentum,
 f_a - velocity distribution function of species a .

Fokker-Planck collision operator

$$C^{ab} = \nu_D^{ab} \mathcal{L}(f_a) + \frac{1}{p^2} \frac{\partial}{\partial p} \left[p^3 \nu_s^{ab} f_a + \frac{1}{2} \nu_{||}^{ab} \frac{\partial f_a}{\partial p} \right]$$


Deflection frequency
(elastic collisions)

Slowing-down
frequency
(inelastic collisions)

Parallel-diffusion
frequency
(parallel-diffusion)

C^{ab} - collision operator for collisions between particle species a and b ,
 $\mathcal{L}(f_a)$ – Lorentz scattering operator,
 p – normalized momentum,
 f_a - velocity distribution function of species a .

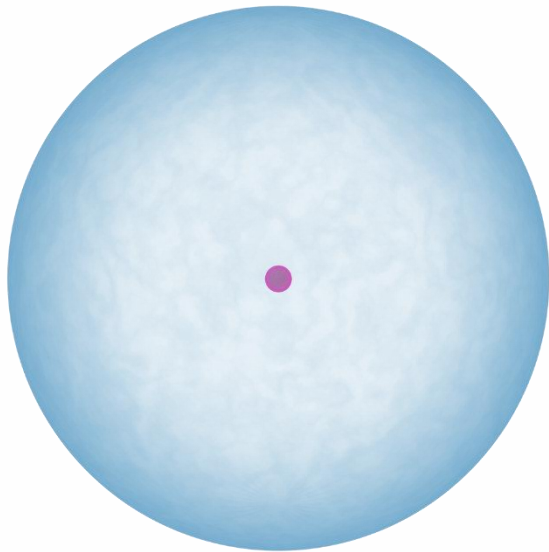


Plasma modeling: elastic collisions – partial screening effect

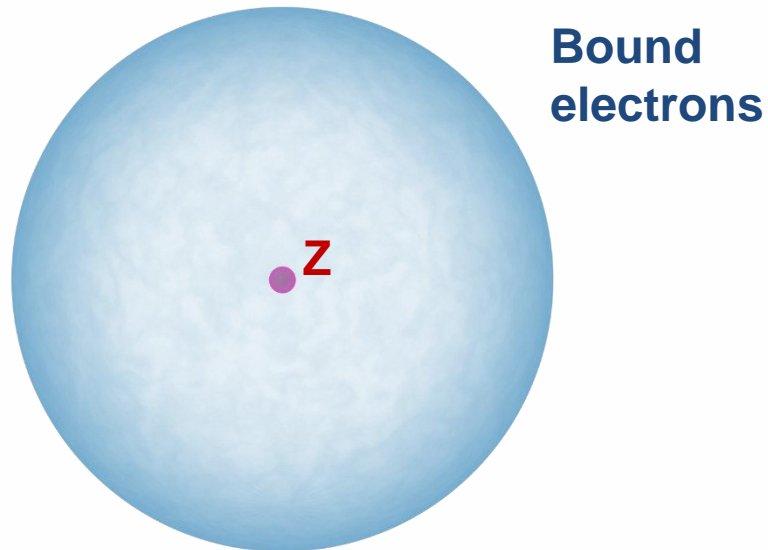
Published in:
Approximate atomic models for fast computation of the Fokker–Planck equation in fusion plasmas with high-Z impurities and suprathermal electrons,

J. Walkowiak et al, *Phys. Plasmas* 29, 022501 (2022)
<https://doi.org/10.1063/5.0075859>

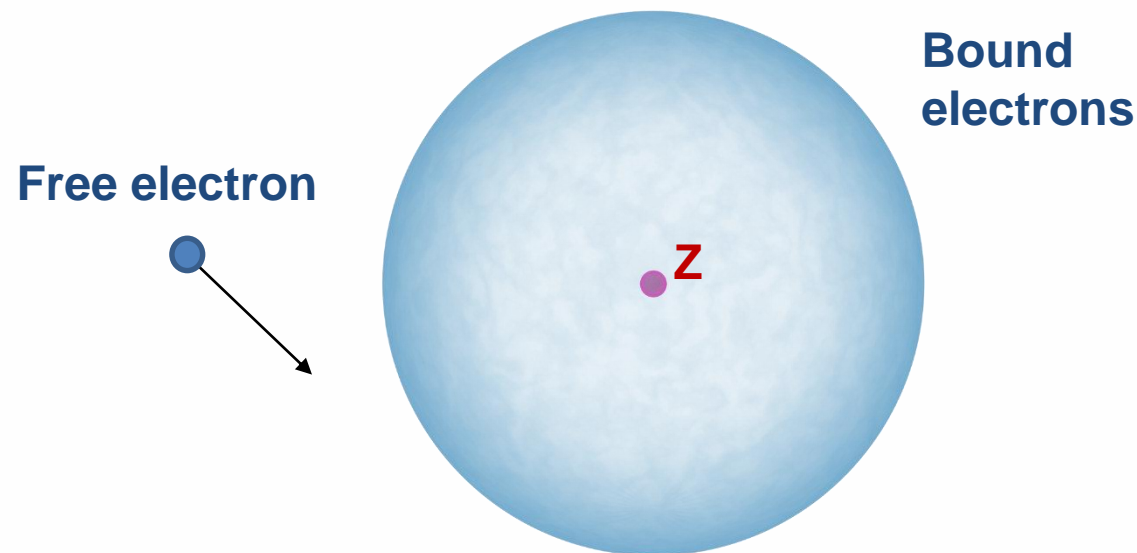
Physical background



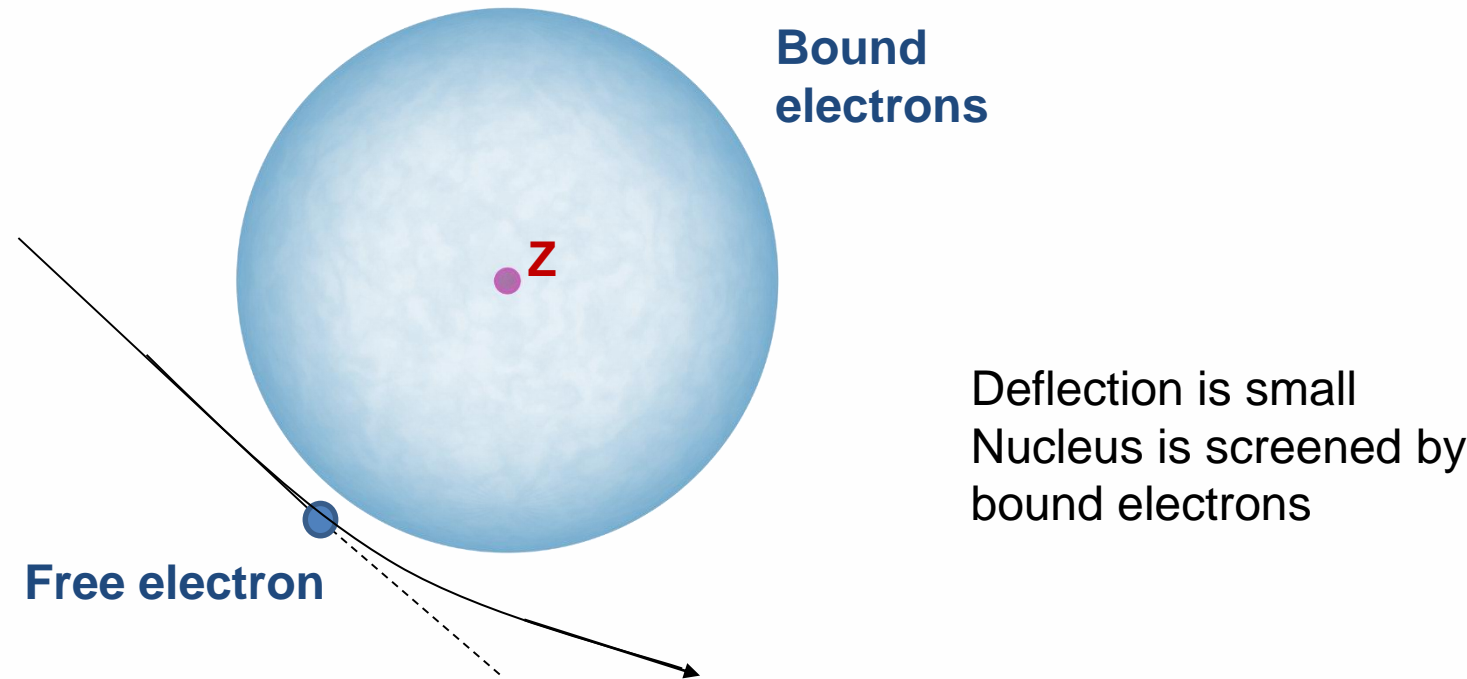
Physical background



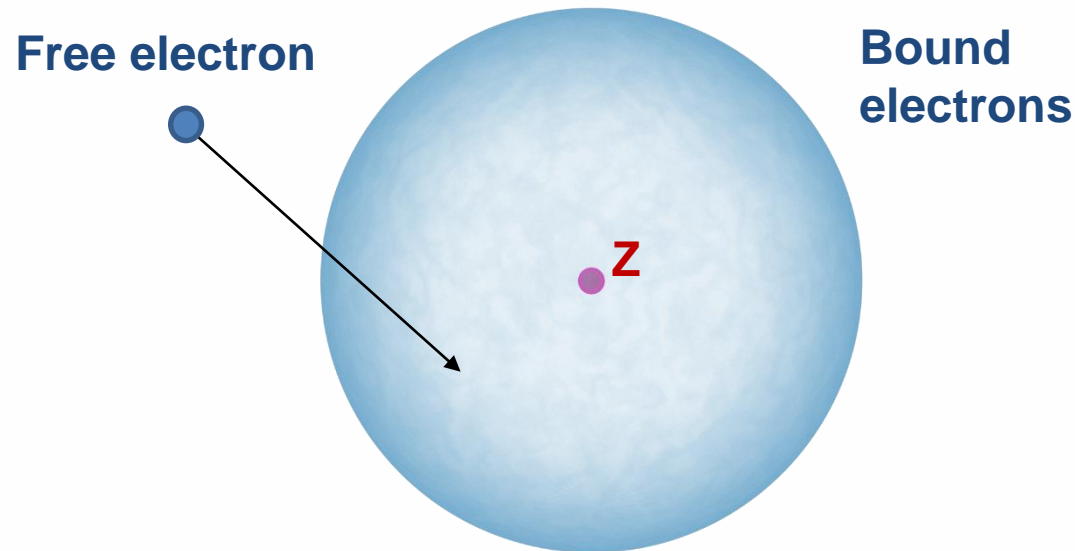
Physical background



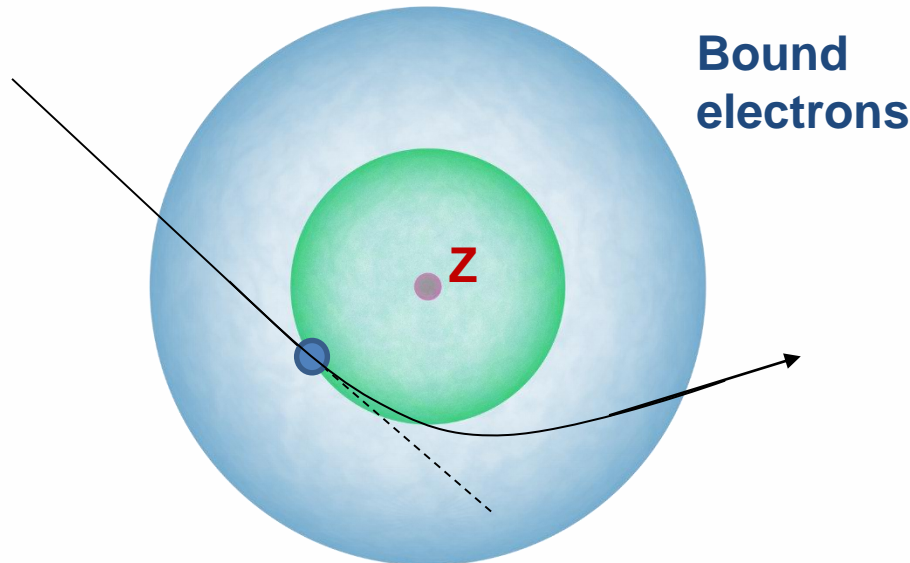
Physical background



Physical background

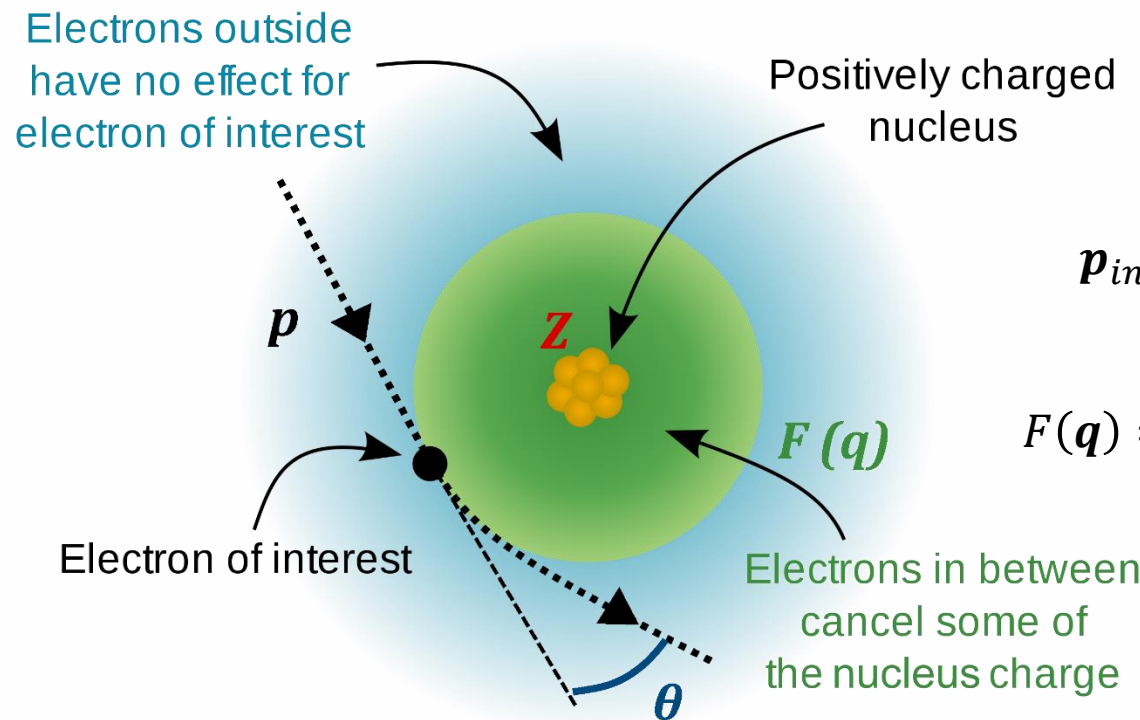


Physical background



Bound
electrons

Physical background



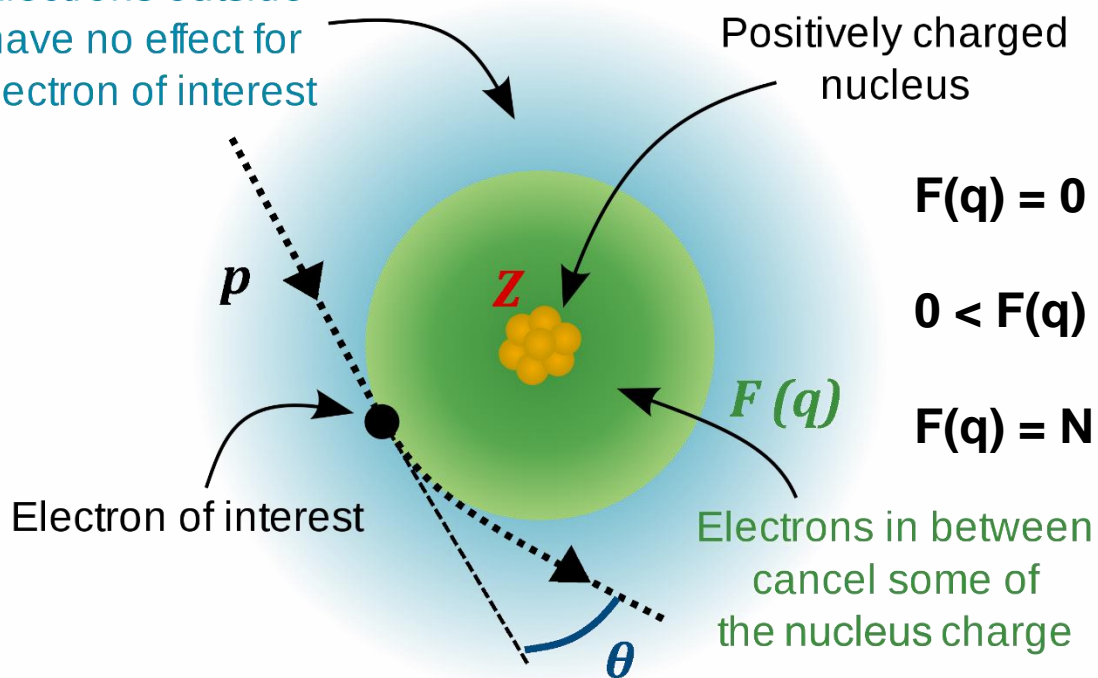
$$\mathbf{p}_{initial} - \mathbf{p}_{final} = \mathbf{q}$$

$$F(\mathbf{q}) = \int \rho(\mathbf{r}) e^{-i\mathbf{qr}/a_0} d^3r$$

Source: A. Jardin et al, 2020 IFJ PAN REPORT NO 2105/AP.
<https://www.ifj.edu.pl/badania/publikacje/raporty/2020/2105.pdf>

Physical background

Electrons outside
have no effect for
electron of interest



$F(q) = 0$

No screening

$0 < F(q) < N$

Partial screening

$F(q) = N$

Full screening

Source: A. Jardin et al, 2020 IFJ PAN REPORT NO 2105/AP.
<https://www.ifj.edu.pl/badania/publikacje/raporty/2020/2105.pdf>

$F(q)$ – atomic form factor
 N – number of bound electrons

Physical background

$$F(q) = \int \rho(r) e^{-iqr/a_0} d^3r$$

↓

Depends on
electron density

$F(q) = 0$

No screening

$0 < F(q) < N$

Partial screening

$F(q) = N$

Full screening

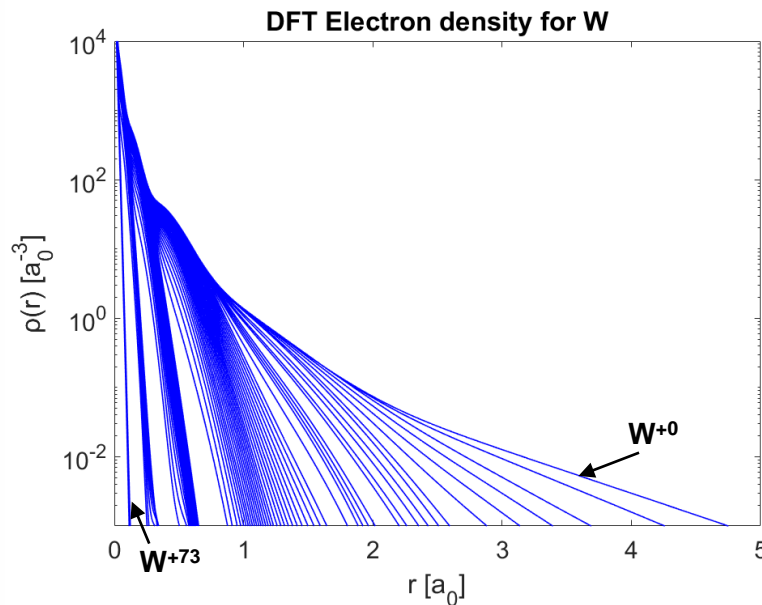
Source: A. Jardin et al, 2020 IFJ PAN REPORT NO 2105/AP.
<https://www.ifj.edu.pl/badania/publikacje/raporty/2020/2105.pdf>

$F(q)$ – atomic form factor
 N – number of bound electrons

Atomic models

Quantum mechanical model

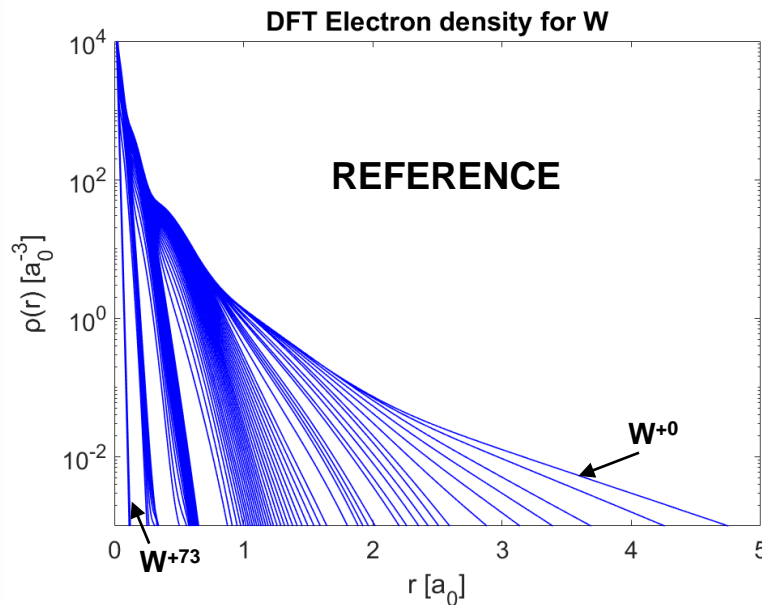
- Density functional theory (DFT)



Atomic models

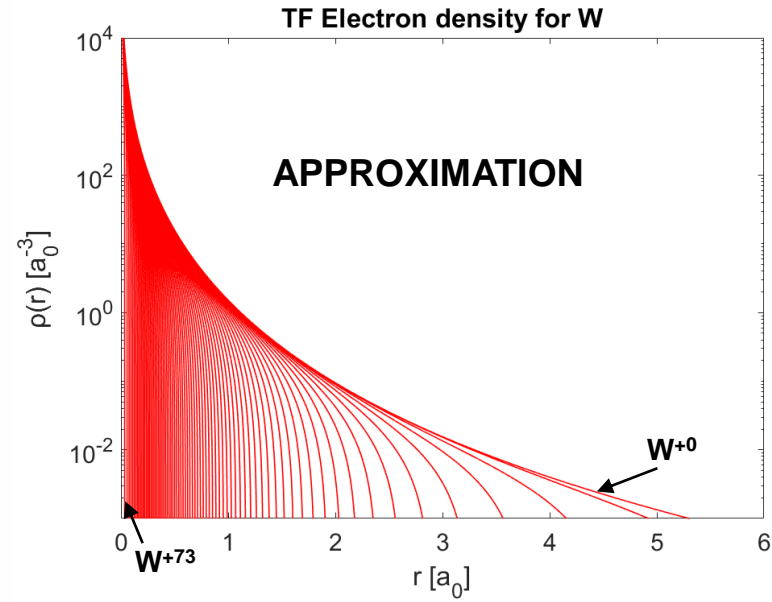
Quantum mechanical model

- Density functional theory (DFT)



Semi-empirical approximations:

- Thomas-Fermi (TF)
- Pratt-Tseng (PT):





Multi-exponential Pratt-Tseng model - PT_opt

Electron density:

$$\rho_{PT}(r) = \frac{N}{4\pi r a^2} \exp\left(-\frac{r}{a}\right)$$

Atomic form factor:

$$F_{PT}(q) = \frac{N}{1 + (qa)^2}$$



Multi-exponential Pratt-Tseng model - PT_opt

Electron density:

$$\rho_{PT}(r) = \frac{N}{4\pi r a^2} \exp\left(-\frac{r}{a}\right)$$

(Yukawa potential)

Atomic form factor:

$$F_{PT}(q) = \frac{N}{1 + (qa)^2}$$



Multi-exponential Pratt-Tseng model - PT_opt

Electron density:

$$\rho_{PT}(r) = \frac{N}{4\pi r a^2} \exp\left(-\frac{r}{a}\right)$$

Atomic form factor:

$$F_{PT}(q) = \frac{N}{1 + (qa)^2}$$



Multi-exponential Pratt-Tseng model - PT_opt

Electron density:

$$\rho_{PT}(r) = \frac{N}{4\pi r a^2} \exp\left(-\frac{r}{a}\right)$$

Atomic form factor:

$$F_{PT}(q) = \frac{N}{1 + (qa)^2}$$



Multi-exponential Pratt-Tseng model - PT_opt

Electron density:

$$\rho_{PT}(r) = \frac{N}{4\pi r a^2} \exp\left(-\frac{r}{a}\right)$$

Atomic form factor:

$$F_{PT}(q) = \frac{N}{1 + (qa)^2}$$

$$\rho_{PT_{opt}}(r) = \frac{1}{4\pi r} \left[\sum_{i=1}^5 \frac{N_i}{a_i^2} \exp\left(-\frac{r}{a_i}\right) \right]$$

(multi Yukawa potential)

Multi-exponential Pratt-Tseng model - PT_opt

Electron density:

$$\rho_{PT}(r) = \frac{N}{4\pi r a^2} \exp\left(-\frac{r}{a}\right)$$

Atomic form factor:

$$F_{PT}(q) = \frac{N}{1 + (qa)^2}$$

$$\rho_{PT_{opt}}(r) = \frac{1}{4\pi r} \left[\sum_{i=1}^5 \frac{N_i}{a_i^2} \exp\left(-\frac{r}{a_i}\right) \right]$$

Multi-exponential Pratt-Tseng model - PT_opt

Electron density:

$$\rho_{PT}(r) = \frac{N}{4\pi r a^2} \exp\left(-\frac{r}{a}\right)$$

Atomic form factor:

$$F_{PT}(q) = \frac{N}{1 + (qa)^2}$$

$$\rho_{PT_{opt}}(r) = \frac{1}{4\pi r} \left[\sum_{i=1}^5 \frac{N_i}{a_i^2} \exp\left(-\frac{r}{a_i}\right) \right]$$



Multi-exponential Pratt-Tseng model - PT_opt

Electron density:

$$\rho_{PT}(r) = \frac{N}{4\pi r a^2} \exp\left(-\frac{r}{a}\right)$$

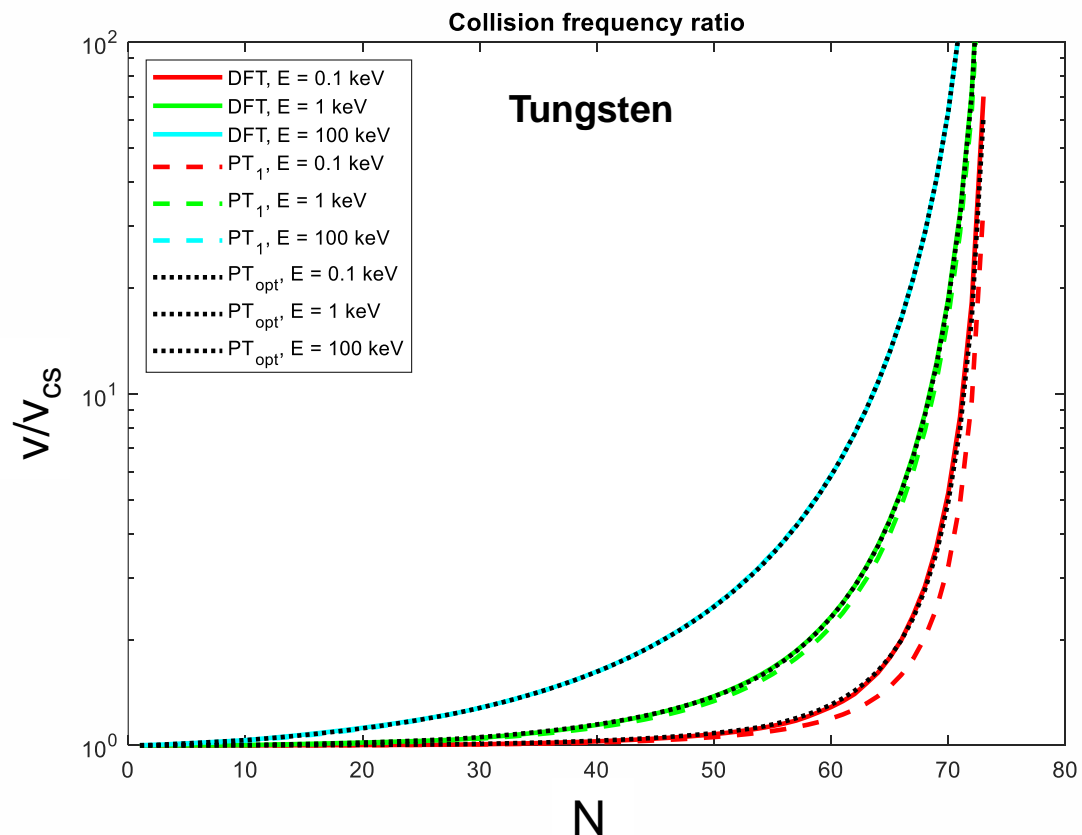
Atomic form factor:

$$F_{PT}(q) = \frac{N}{1 + (qa)^2}$$

$$\rho_{PT_{opt}}(r) = \frac{1}{4\pi r} \left[\sum_{i=1}^5 \frac{N_i}{a_i^2} \exp\left(-\frac{r}{a_i}\right) \right]$$

$$F_{PT_{opt}}(q) = \sum_{i=1}^5 \frac{N_i}{1 + (qa_i)^2}$$

Results: elastic collision frequency



DESCRIPTION

- The elastic collision frequency ratio calculated for tungsten ions
- Collision frequency ratio = partial screening / complete screening case
- Coulomb logarithm $\ln \Lambda = 16.3$ (plasma electron density $n_e = 5 \cdot 10^{19} \text{ m}^{-3}$ and electron temperature $T_e = 3 \text{ keV}$)



Plasma modeling: inelastic collisions

Planned to be published as:
Mean excitation energy of all ions of elements up to Radon
Submission planned at March/April 2024
to Physical Review E



Inelastic collisions - Stopping power

Formal definition:

$$S(v) = -\frac{1}{n} \frac{dE(v)}{dx}$$

$S(v)$ – stopping power

$E(v)$ – particle kinetic energy

v – particle velocity

n – scatter density

x – length of the particle trajectory

Inelastic collisions - Stopping power

Formal definition:

$$S(v) = -\frac{1}{n} \frac{dE(v)}{dx}$$

Bethe-Bloch theory (with further corrections) [ICRU Report 1984]:

$$S(v) = \frac{4\pi e^4}{mv^2} N \left[\ln \frac{2mv^2}{I} - \beta^2 - \frac{\delta}{2} - \frac{U}{2} \right]$$

$S(v)$ – stopping power

$E(v)$ – particle kinetic energy

v – particle velocity

n – scatter density

x – length of the particle trajectory

N – number of bound electrons in target atoms

$\beta = v/c$ - relativistic correction

δ – density-effect correction factor

U – shell-effect correction factor

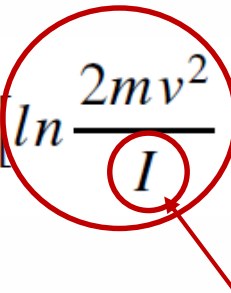
Source: ICRU Report 49, Stopping Powers and Ranges for Protons and Alpha Particles (1984).

Inelastic collisions - Stopping power

Formal definition:

$$S(v) = -\frac{1}{n} \frac{dE(v)}{dx}$$

Bethe-Bloch theory (with further corrections) [ICRU Report 1984]:

$$S(v) = \frac{4\pi e^4}{mv^2} N \left[\ln \frac{2mv^2}{I} - \beta^2 - \frac{\delta}{2} - \frac{U}{2} \right]$$


Mean excitation energy

Source: ICRU Report 49, Stopping Powers and Ranges for Protons and Alpha Particles (1984).



Mean Excitation Energy

$$\ln(MEE) = \frac{\int f \frac{df}{dE} \ln E dE}{\int f \frac{df}{dE} dE}$$

$\ln(MEE)$ – natural logarithm of Mean Excitation Energy

E - energy of transition

f - oscillator strength of transition

Mean Excitation Energy

$$\ln(MEE) = \frac{df}{dE} \ln E dE / \int \frac{df}{dE} dE$$

$$\ln(MEE) \approx \frac{4\pi}{N} \int r^2 \rho(r) \ln(\hbar\omega_0(r)) dr + \exp\left(\frac{Z-N}{Z}\right) - 0.9$$

$$\omega_o = \sqrt{4\pi e^2 \rho(r)/m}$$

$\ln(MEE)$ – natural logarithm of Mean Excitation Energy
 E_{n0} - energy of transition $0 \rightarrow n$
 f_{n0} - oscillator strength of transition $0 \rightarrow n$

ω_0 - local plasma frequency
 r - atomic radius
 \hbar – reduced Planck constant

Z – atomic number
 N - number of bound electrons
 $\rho(r)$ – electron density in ion

Mean Excitation Energy

$$\ln(MEE) = \sum \frac{df}{dE} \ln E dE / \sum \frac{df}{dE} dE$$
$$\ln(MEE) \approx \frac{4\pi}{N} \int r^2 \rho(r) \ln(\hbar\omega_0(r)) dr + \exp\left(\frac{Z-N}{Z}\right) - 0.9$$

Local Plasma Approximation

$$\omega_o = \sqrt{4\pi e^2 \rho(r)/m}$$

$\ln(MEE)$ – natural logarithm of Mean Excitation Energy

E_{n0} - energy of transition $0 \rightarrow n$

f_{n0} - oscillator strength of transition $0 \rightarrow n$

ω_0 - local plasma frequency

r - atomic radius

\hbar – reduced Planck constant

Z – atomic number

N - number of bound electrons

$\rho(r)$ – electron density in ion

Mean Excitation Energy (MEE)

$$\ln(MEE) = \frac{df}{dE} \ln E dE / \int \frac{df}{dE} dE$$

$$\ln(MEE) \approx \frac{4\pi}{N} \int r^2 \rho(r) \ln(\hbar\omega_0(r)) dr + \exp\left(\frac{Z-N}{Z}\right) - 0.9$$

$$\omega_o = \sqrt{4\pi e^2 \rho(r)/m}$$

**Free parameter
replaced with fit function**

$\ln(MEE)$ – natural logarithm of Mean Excitation Energy

E_{n0} - energy of transition $0 \rightarrow n$

f_{n0} - oscillator strength of transition $0 \rightarrow n$

ω_0 - local plasma frequency

r - atomic radius

\hbar – reduced Planck constant

Z – atomic number

N - number of bound electrons

$\rho(r)$ – electron density in ion



Mean Excitation Energy (MEE)

Local plasma approximation [Lindhard 1953] (LPA):

$$\ln I = \frac{1}{N} \int d^3r 4\pi r^2 \rho(r) \ln(\gamma \hbar \omega_0)$$

$$\omega_o = \sqrt{4\pi e^2 \rho(r)/m}$$

$\ln I$ - mean excitation energy

E_{n0} - energy of transition $0 \rightarrow n$

f_{n0} - oscillator strength of transition $0 \rightarrow n$

ω_0 - local plasma frequency

r - atomic radius

\hbar - reduced Planck constant

Source: J. Lindhard and M. Scharff, K. Dan. Vidensk. Selsk. Mat. Fys. Medd. 27 (1953) no. 15.

Mean Excitation Energy (MEE)

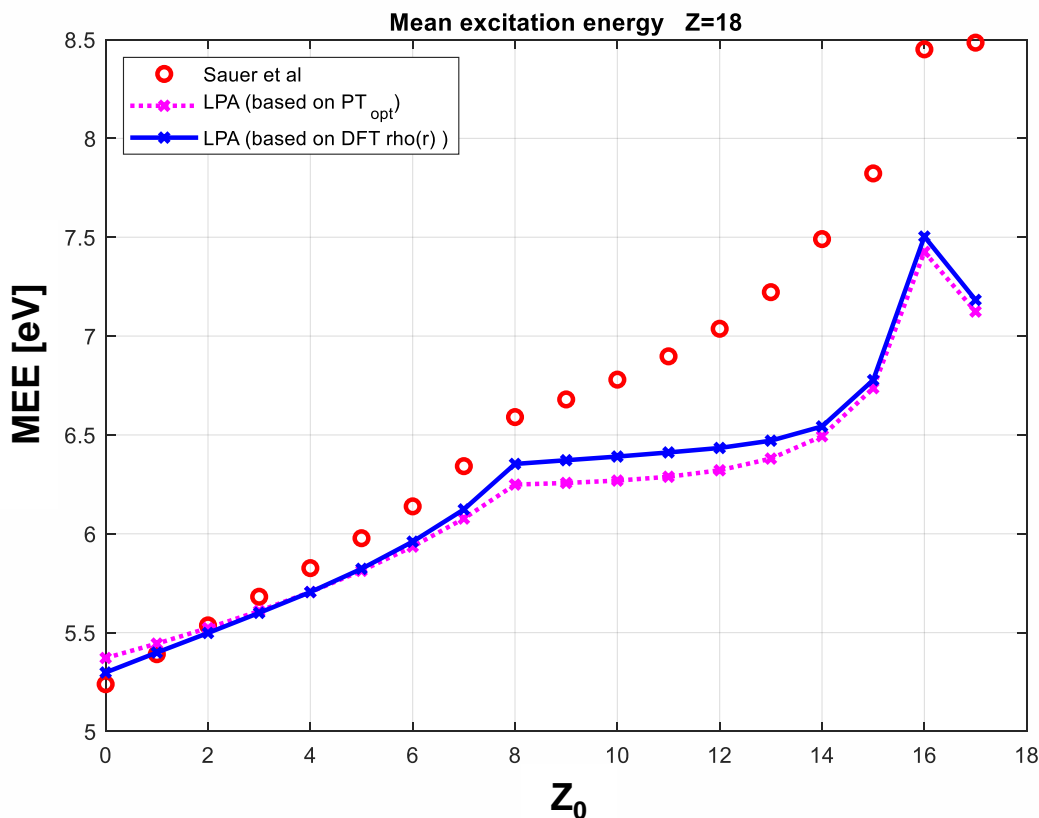
Local plasma approximation [Lindhard 1953] (LPA):

$$\ln I = \frac{1}{N} \int d^3r 4\pi r^2 \rho(r) \ln(\gamma \hbar \omega_0)$$
$$\omega_o = \sqrt{4\pi e^2 \rho(r) / m_e}$$

Depends on
electron density

Source: J. Lindhard and M. Scharff, K. Dan. Vidensk. Selsk. Mat. Fys. Medd. 27 (1953) no. 15.

Results – Local Plasma Approximation



Source: [Sauer 2015]

DESCRIPTION

- LPA calculations based on different models of electron density, compared to MCSCF RPA calculations by Sauer et.al

LPA equation:

$$\ln I = \frac{4\pi}{N} \int r^2 \rho(r) \ln(\hbar\omega_0) dr + \\ + \ln(\sqrt{2})$$

Mean excitation energy

Local plasma approximation [Lindhard 1953] (LPA):

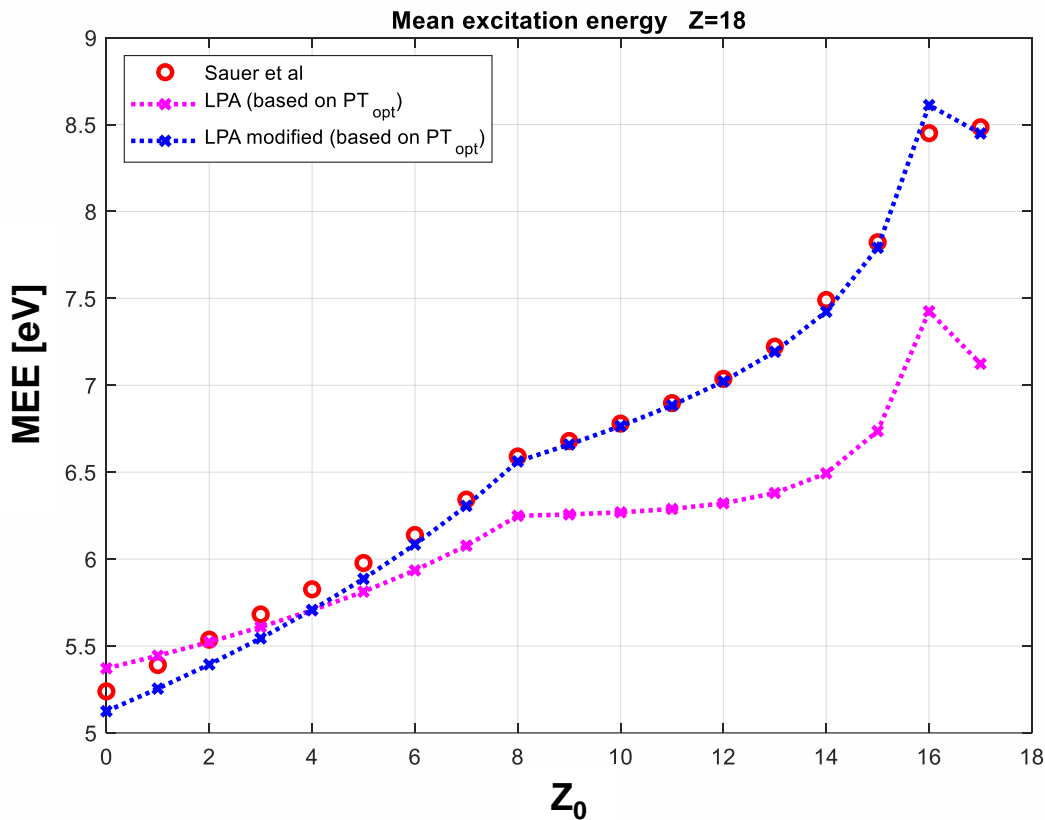
$$\ln I = \frac{1}{N} \int d^3r 4\pi r^2 \rho(r) \ln(\gamma \hbar \omega_0)$$

Main sources of discrepancy:

- Lindhard model is based on the TF atomic model, which is not accurate for innermost electrons
- The γ constant is not precisely defined

Source: J. Lindhard and M. Scharff, K. Dan. Vidensk. Selsk. Mat. Fys. Medd. 27 (1953) no. 15.

Results – Local Plasma Approximation



Source: [Sauer 2015]

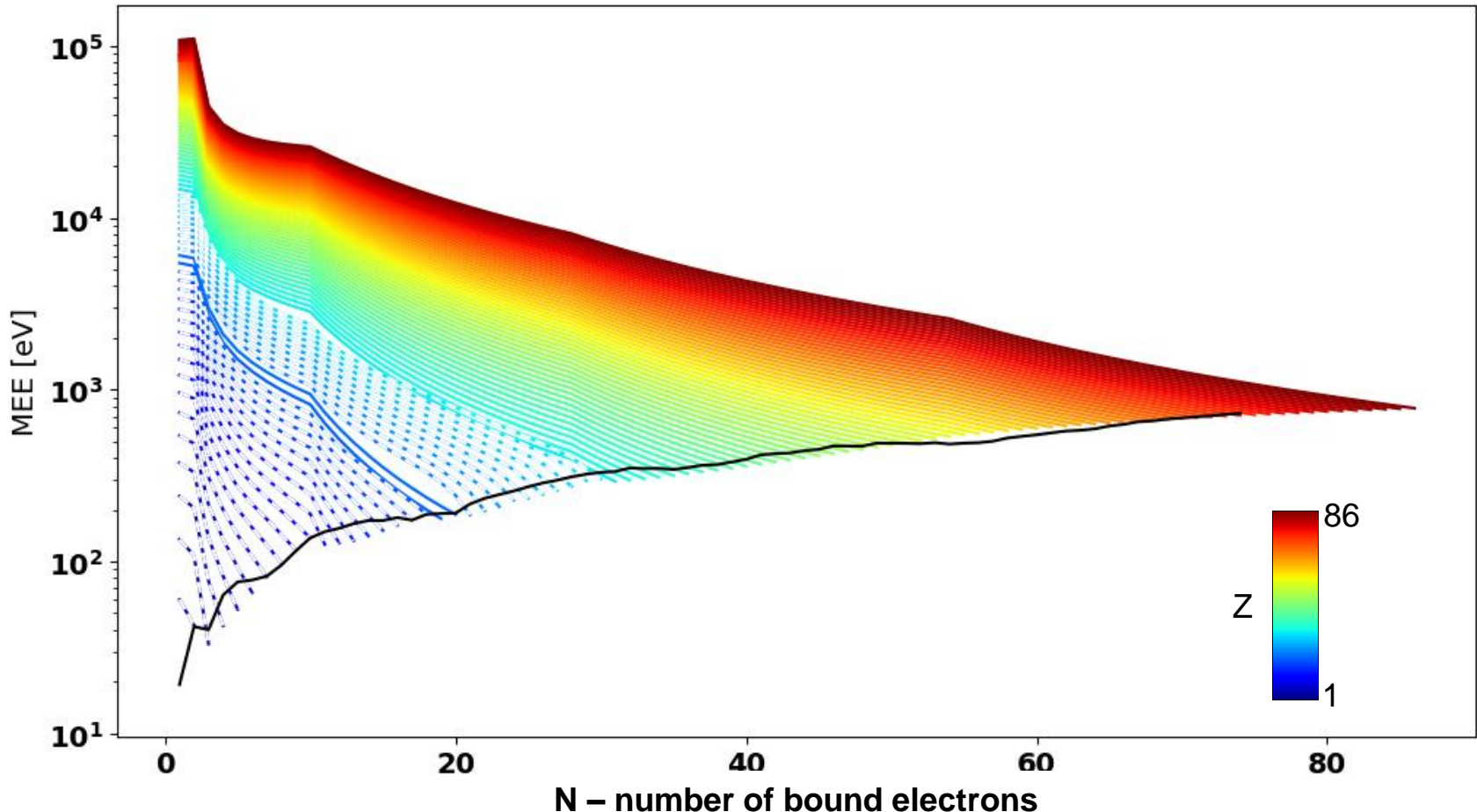
DESCRIPTION

- LPA calculations with ad hoc correction, compared to MCSCF RPA by Sauer et.al

Modified LPA equation:

$$\ln I = \frac{4\pi}{N} \int r^2 \rho(r) \ln(\hbar\omega_0) dr + \\ + \exp\left(\frac{Z - N}{Z}\right) - 0.9$$

Mean Excitation Energy





Disruption modelling

Published in:

First numerical analysis of runaway electron generation in tungsten-rich plasmas towards ITER,

J. Walkowiak et al, *Nucl. Fusion* **64**, 036024 (2024)

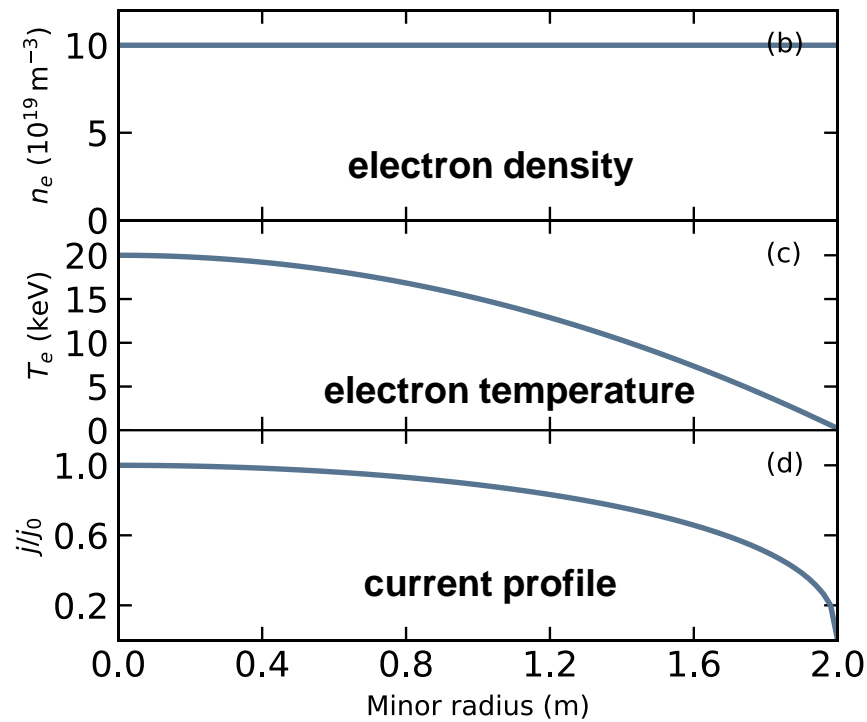
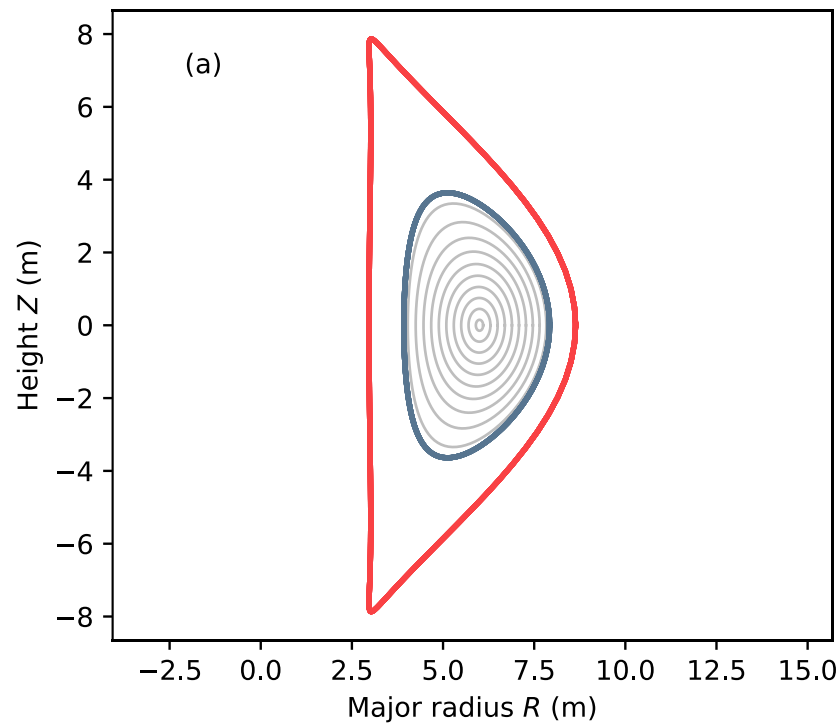
<https://iopscience.iop.org/article/10.1088/1741-4326/ad24a0>



Source: M. Hoppe et al, 2021, Comput. Phys. Commun. 268 108098

Simulation setup

Magnetic surfaces

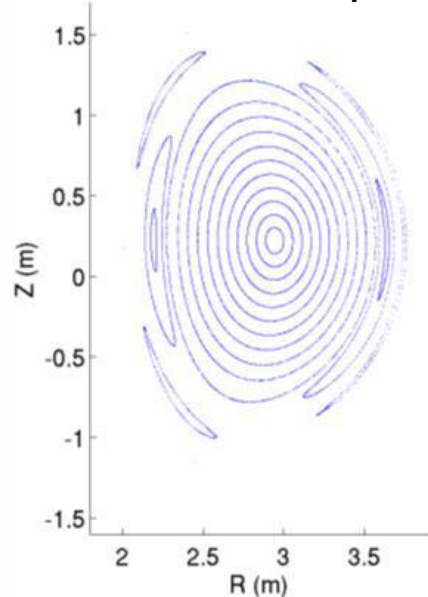


Source: J. Walkowiak *et al* 2024 *Nucl. Fusion* 64 036024

Disruption

Stages:

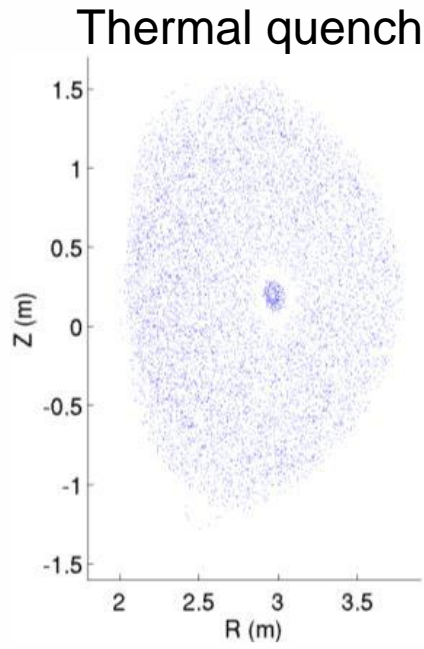
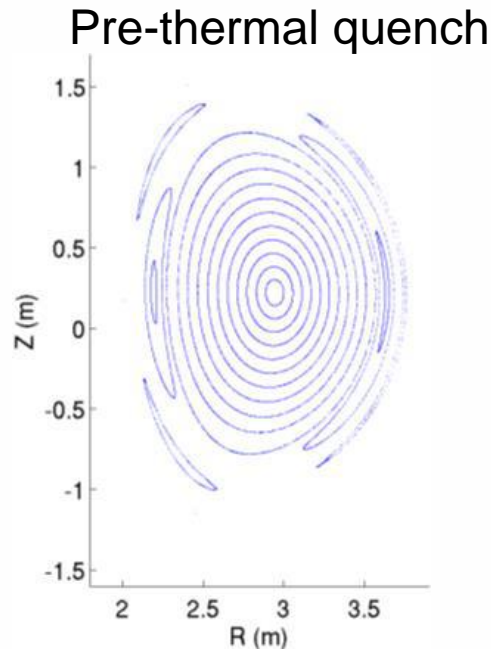
Pre-thermal quench



Source: C. Sommariva et al. (2006) 43rd EPS Conference on Plasma Physics

Disruption

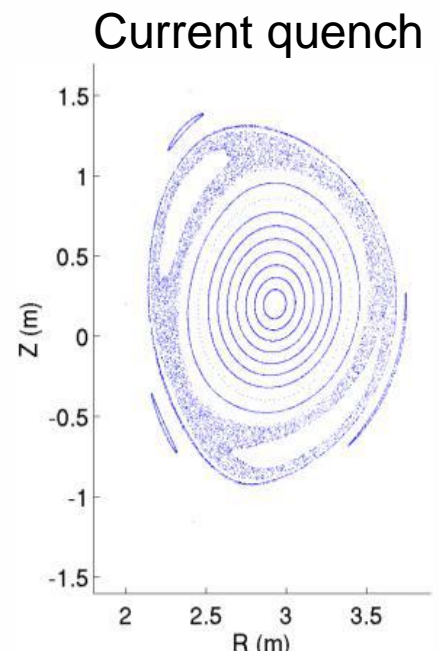
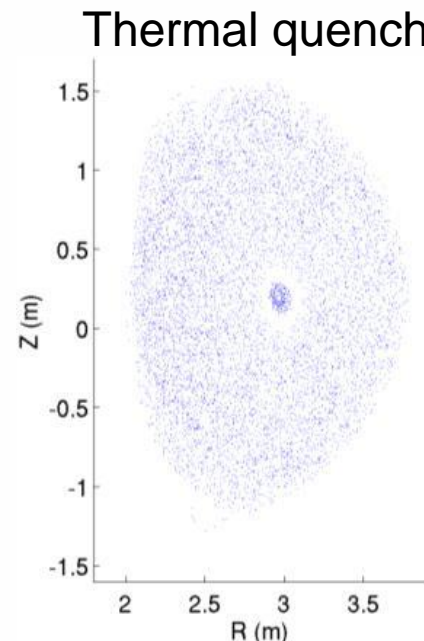
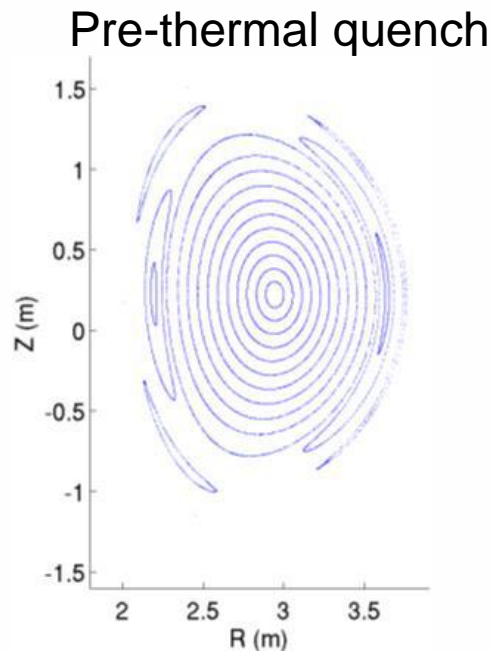
Stages:



Source: C. Sommariva et al. (2006) 43rd EPS Conference on Plasma Physics

Disruption

Stages:

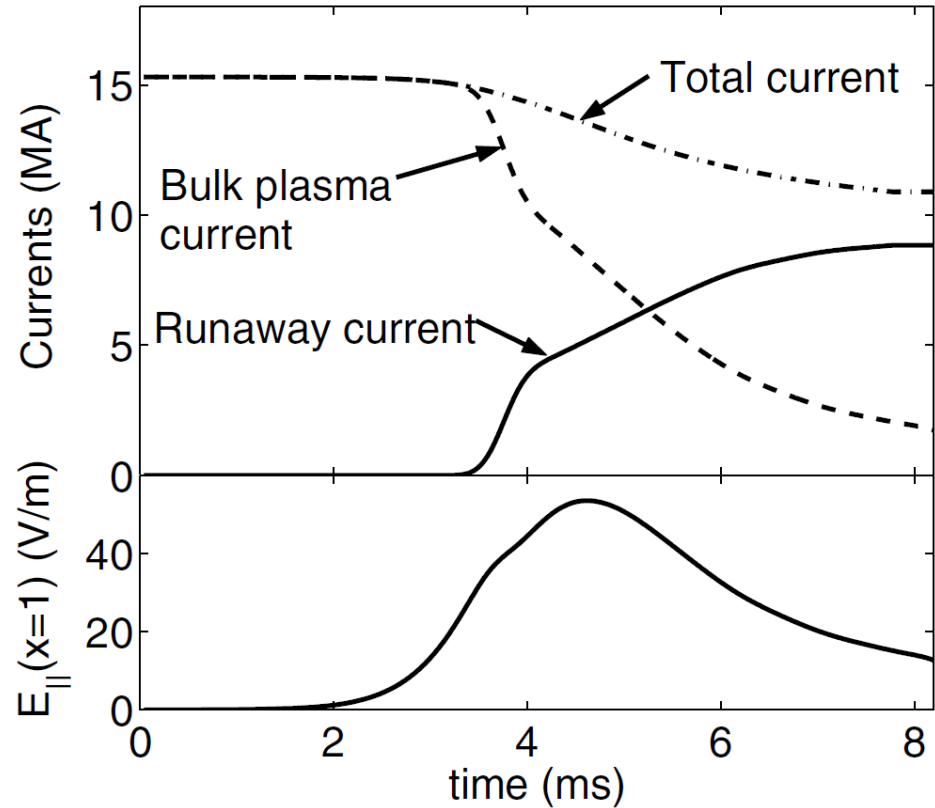


Source: C. Sommariva et al. (2006) 43rd EPS Conference on Plasma Physics

Disruption

Stages:

- Thermal quench (TQ)
- Current quench (CQ)



Source: L.-G. Eriksson et al. (2004) Phys. Rev. Lett. 92, 205004

Disruption

Stages:

- Thermal quench (TQ)
- Current quench (CQ)

Safety requirements of ITER:

- **Runaway electrons current < 150 kA**
- $50\text{ms} < \text{Current quench time} < 150\text{ms}$



Source: E. Joffrin et al, 5th REM meeting 2017

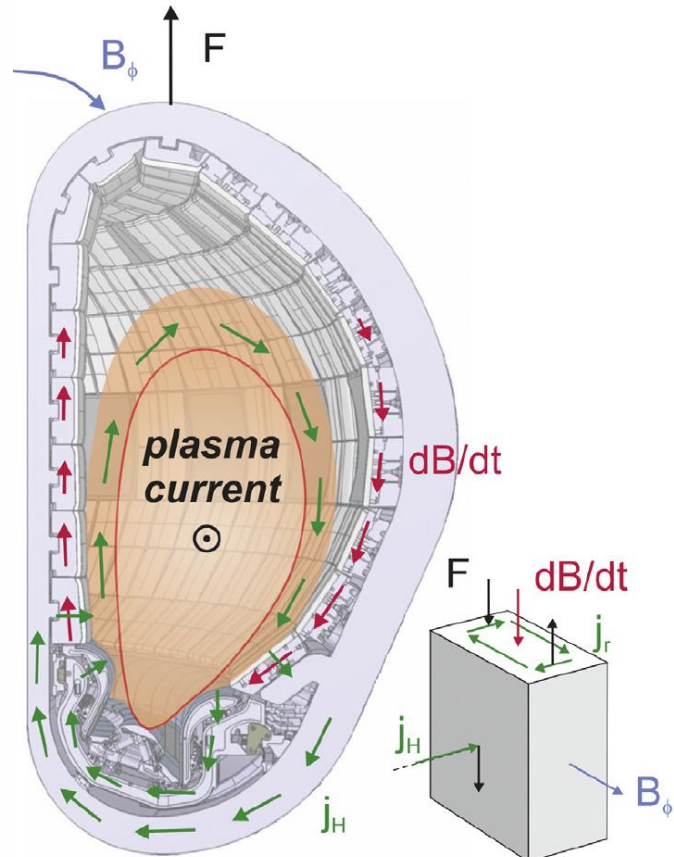
Disruption

Stages:

- Thermal quench (TQ)
- Current quench (CQ)

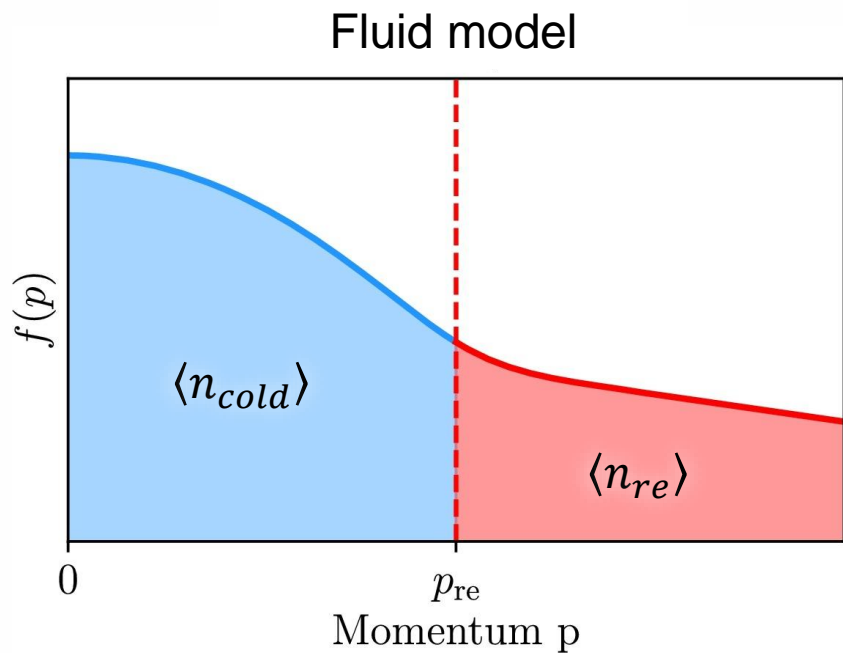
Safety requirements of ITER:

- Runaway electrons current < 150 kA
- **50ms < Current quench time < 150ms**



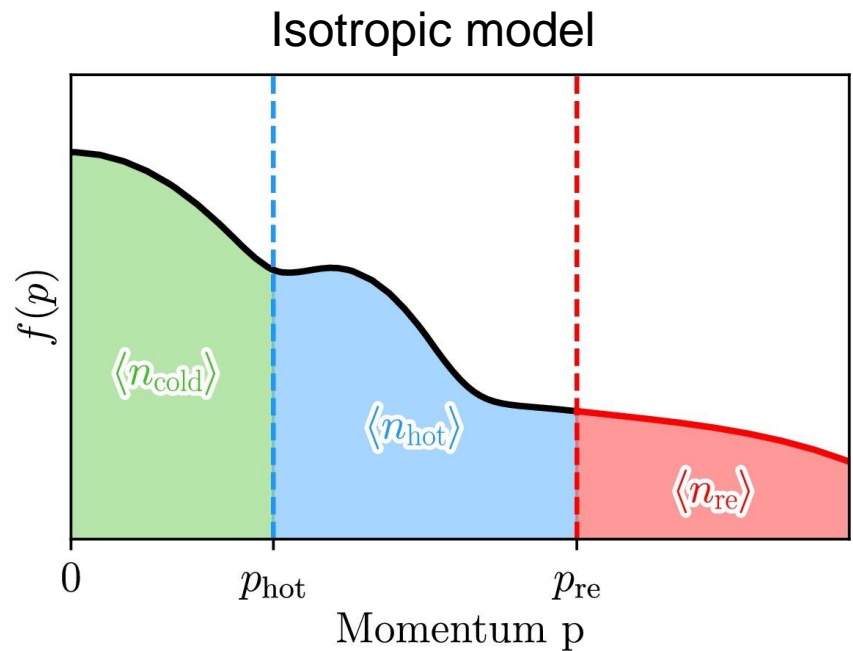
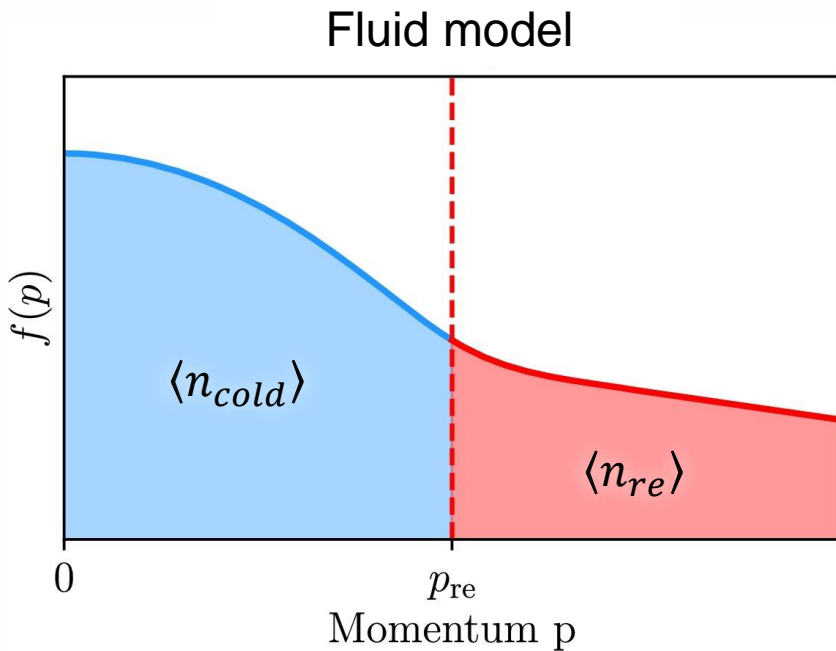
Source: Lehnert M. et al 2015 J. Nucl. Mater. **463** 39–48

Fluid and isotropic model



Source: M. Hoppe et al, 2021, Comput. Phys. Commun. 268 108098

Fluid and isotropic model



Source: M. Hoppe et al, 2021, Comput. Phys. Commun. 268 108098



Parameter scan to assess uncertainties

Tungsten (W) concentration:

Magnetic perturbation (dB/B0):



Parameter scan to assess uncertainties

Tungsten (W) concentration:

- Tungsten is deposited instantaneously at the beginning of the simulation with concentration uniform in radius.
- There is no tungsten transport in the simulation.

Magnetic perturbation (dB/B0):

Parameter scan to assess uncertainties

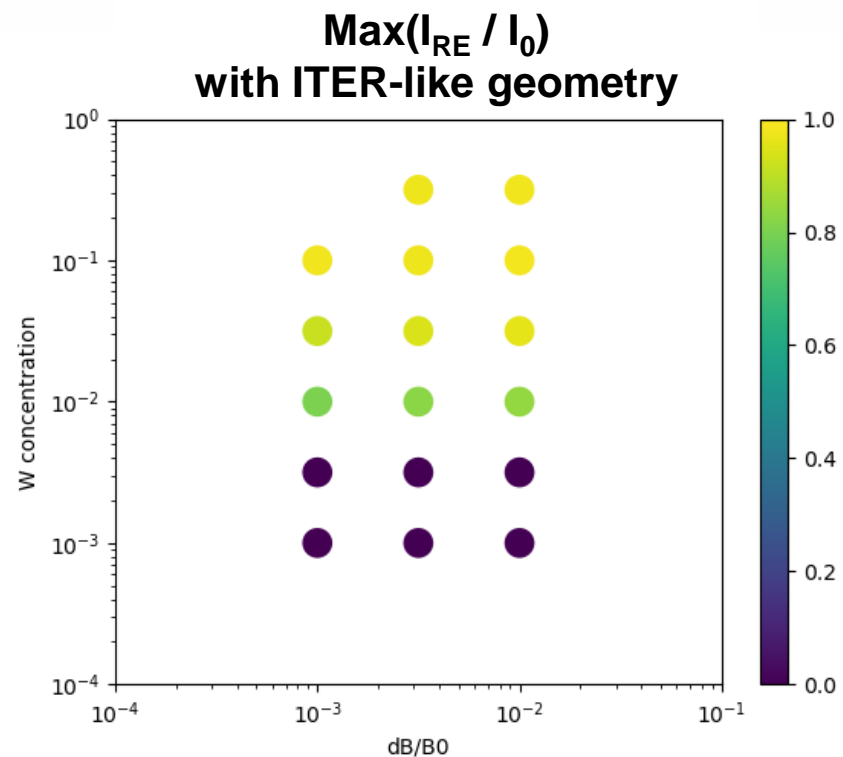
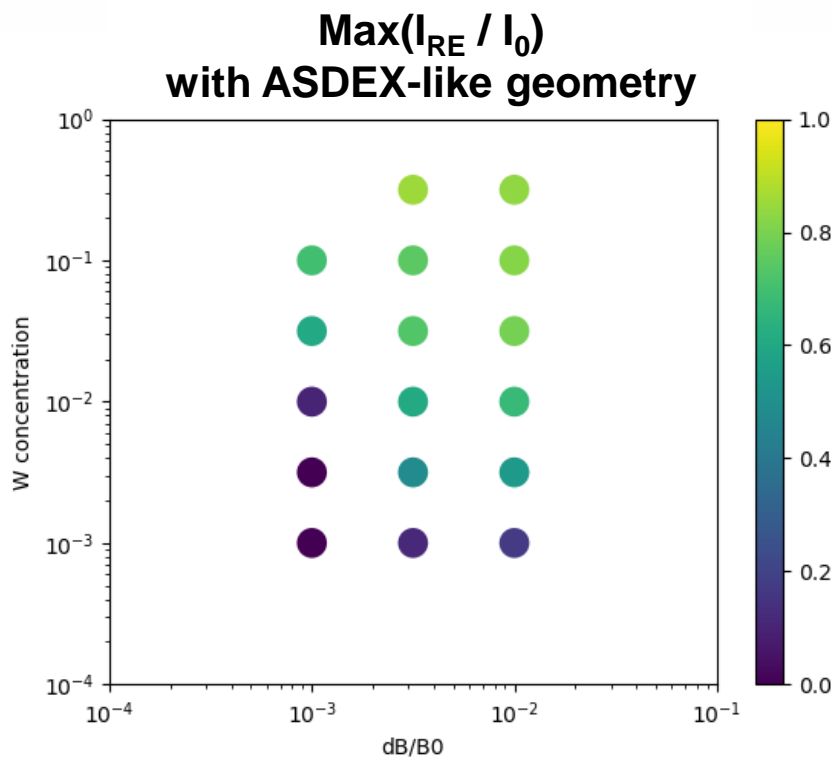
Tungsten (W) concentration:

- Tungsten is deposited instantaneously at the beginning of the simulation with concentration uniform in radius.
- There is no tungsten transport in the simulation.

Magnetic perturbation (dB/B0):

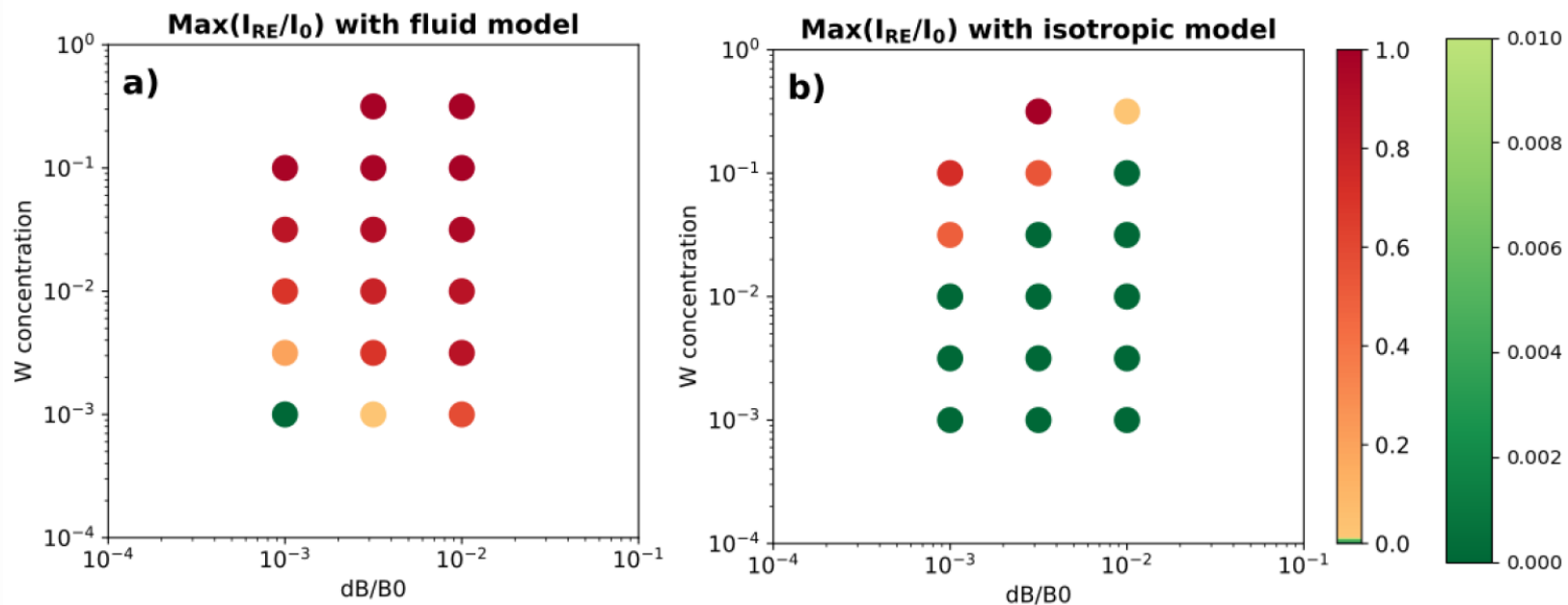
- Simulation is divided into two steps: thermal quench (TQ) and current quench (CQ).
- Main difference between them is the strength of the magnetic perturbation applied (which affects diffusion coefficients for heat transfer and RE)

Results: ASDEX-like (medium) vs ITER-like (large)



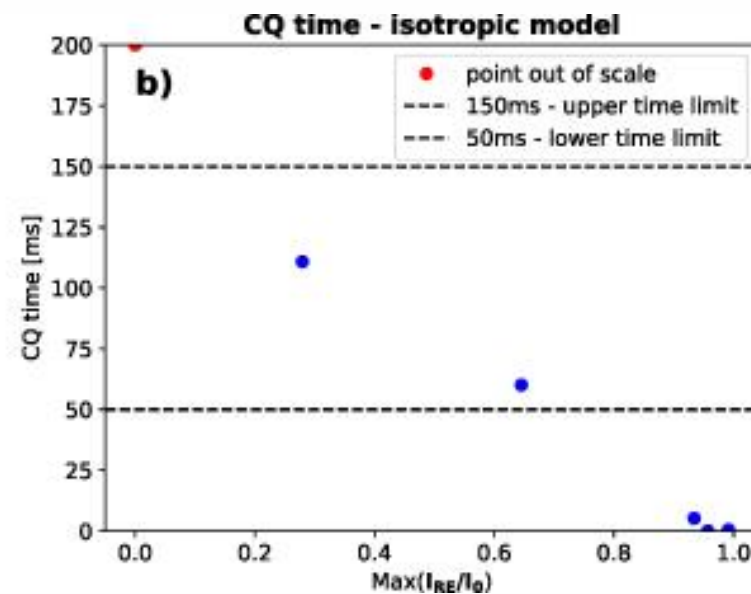
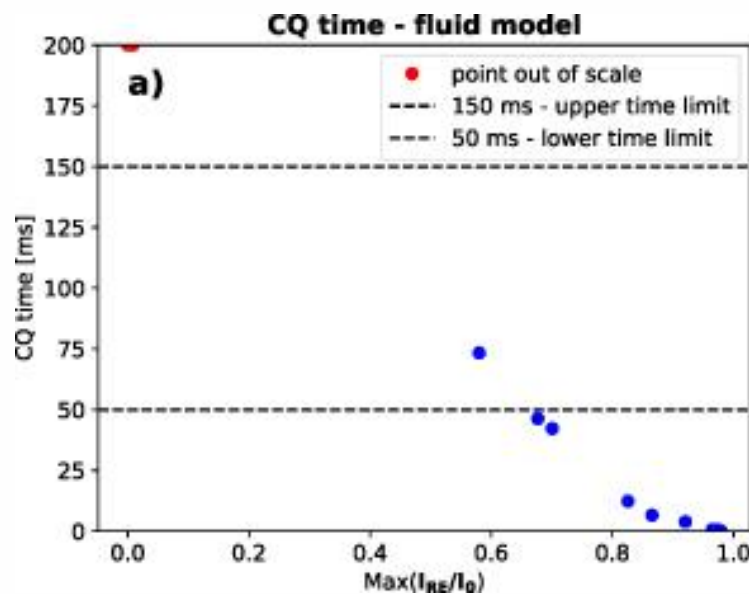
Source: J. Walkowiak et al 2024 *Nucl. Fusion* 64 036024

Results: fluid vs isotropic (kinetic) model



Source: J. Walkowiak et al 2024 *Nucl. Fusion* 64 036024

Results of Current Quench (CQ) time: fluid vs isotropic



Source: J. Walkowiak et al 2024 *Nucl. Fusion* 64 036024



Conclusions

- With W concentrations usually observed in tokamaks ($< 10^{-3}$), W impurities are probably not enough to generate significant RE current



Conclusions

- With W concentrations usually observed in tokamaks ($< 10^{-3}$), W impurities are probably not enough to generate significant RE current
- Further validation is needed to evaluate the above statement



Conclusions

- With W concentrations usually observed in tokamaks ($< 10^{-3}$), W impurities are probably not enough to generate significant RE current
- Further validation is needed to evaluate the above statement
- W impurities can significantly shorten CQ time and make it more difficult to keep it in the safety limit (50 ms - 150 ms)



Conclusions

- With W concentrations usually observed in tokamaks ($< 10^{-3}$), W impurities are probably not enough to generate significant RE current
- Further validation is needed to evaluate the above statement
- W impurities can significantly shorten CQ time and make it more difficult to keep it in the safety limit (50 ms - 150 ms)

Perspectives

- Impact of the tungsten impurities on runaway electrons mitigation system
- Runaway electrons termination with high-Z impurities



Summary

- Extensive work on atomic physics was done, to support modeling of electron dynamics in plasma with tungsten impurities



Summary

- Extensive work on atomic physics was done, to support modeling of electron dynamics in plasma with tungsten impurities
- Results were implemented in the DREAM code, which is used for safety analysis of tokamaks in terms of runaway electrons generation



Summary

- Extensive work on atomic physics was done, to support modeling of electron dynamics in plasma with tungsten impurities
- Results were implemented in the DREAM code, which is used for safety analysis of tokamaks in terms of runaway electrons generation
- Main value of this work is delivering simulation tools for further tokamak analysis, which can include tungsten impurities in runaway mitigation scenarios



Team

- Supervisor: Jakub Bielecki
- Co-supervisor: Axel Jardin
- Harmonia team (IFJ):
Marek Scholz, Krzysztof Król, Dominik Dworak
- CEA collaboration:
Yves Savoye-Peysson, Didier Mazon
- Chalmers collaboration:
Mathias Hoppe, Tünde Fülöp, István Pusztai, Ida Ekmark, Oskar Vallhagen
- Special thanks to prof. Jacek Bieroń (UJ)



Papers

- J.Walkowiak et al, **Approximate atomic models for fast computation of the Fokker–Planck equation in fusion plasmas with high-Z impurities and suprathermal electrons**, *Phys. Plasmas* 29, 022501, 2022
<https://doi.org/10.1063/5.0075859>
- J.Walkowiak et al, **First numerical analysis of runaway electron generation in tungsten-rich plasmas towards ITER**, *Nucl. Fusion* 64, 036024, 2024
<https://iopscience.iop.org/article/10.1088/1741-4326/ad24a0>
- J.Walkowiak et al, **Mean excitation energy of all ions of elements up to Radon – to be published**

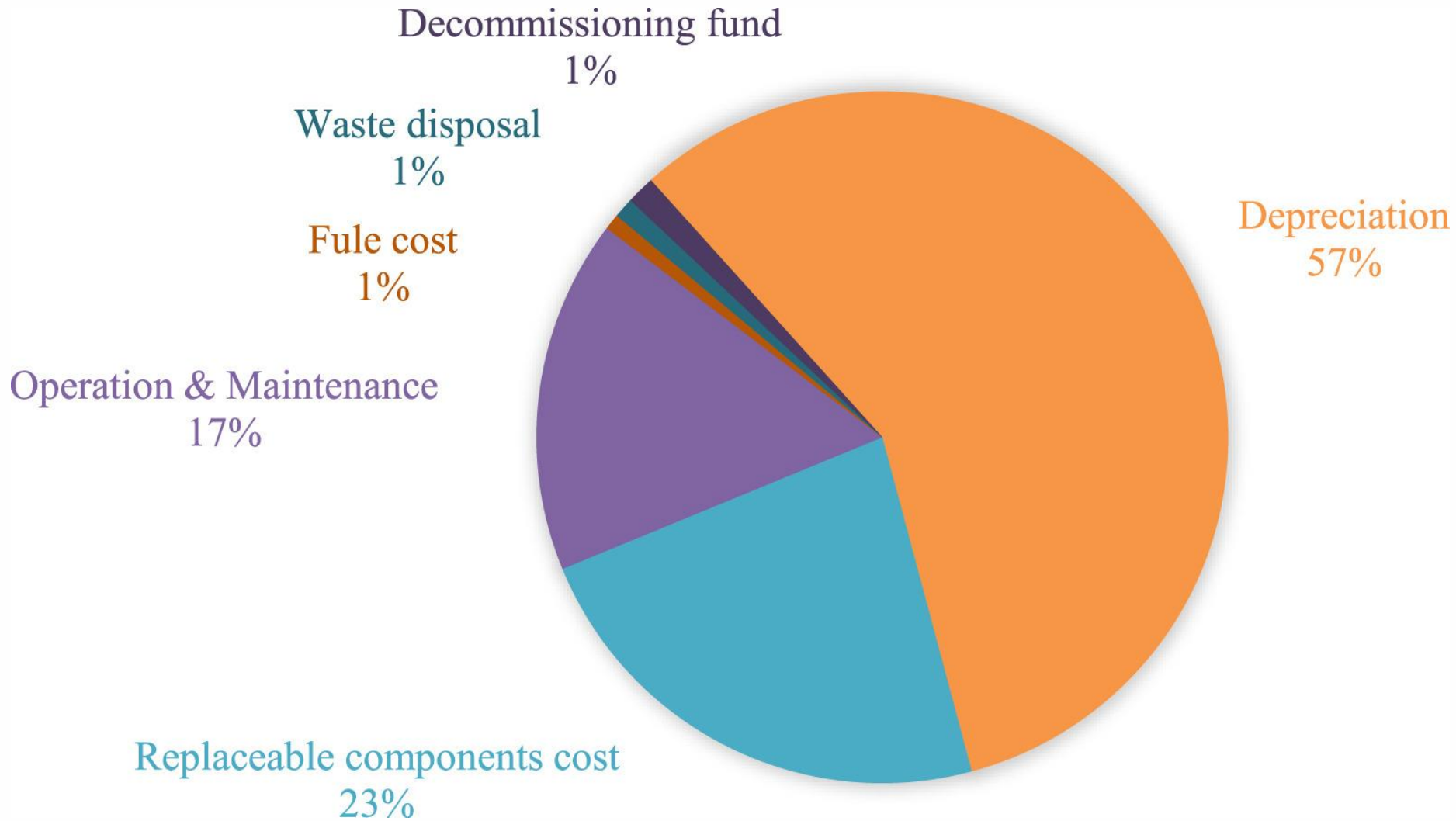


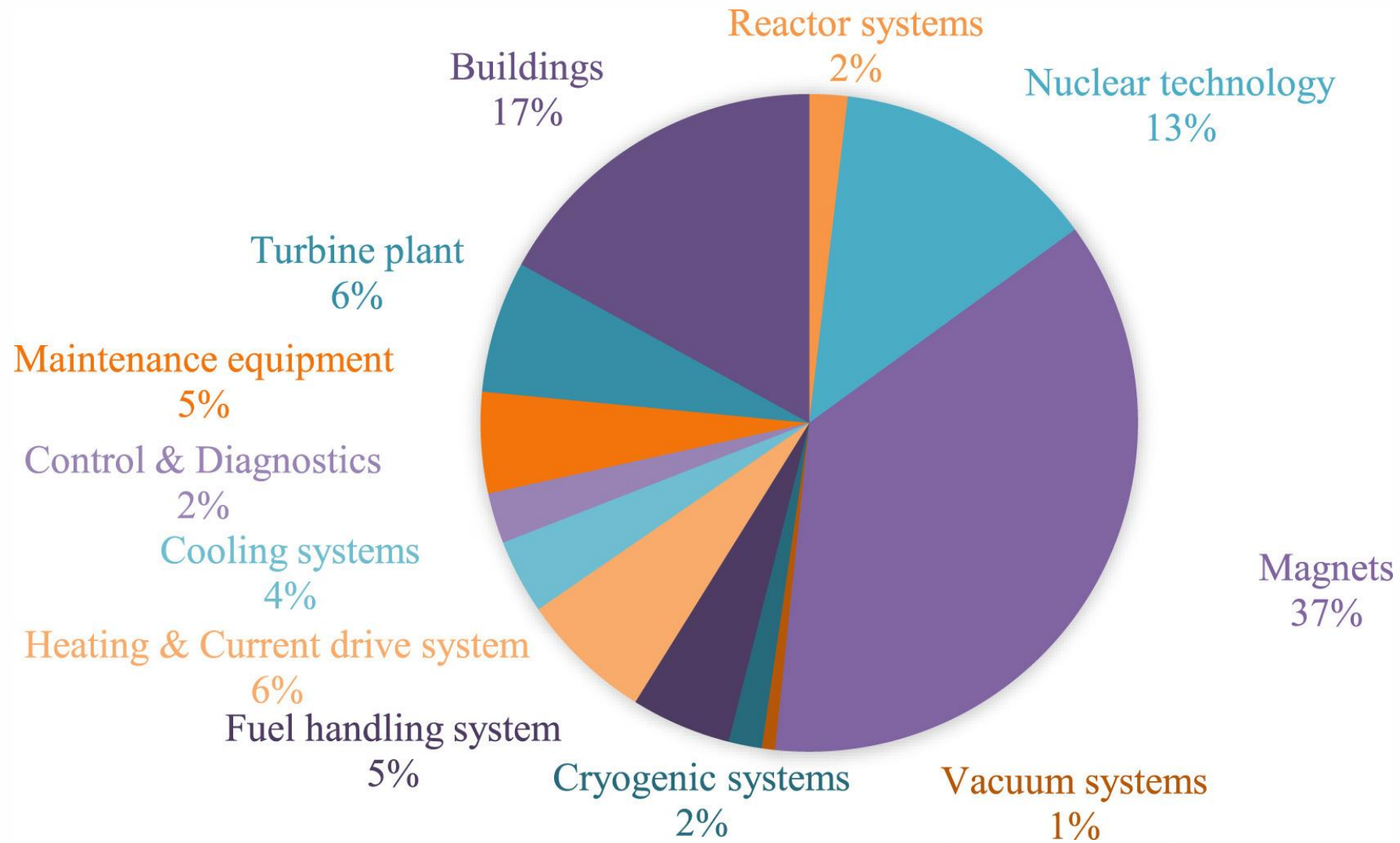
Acknowledgment

- This work has been partially funded by the National Science Centre, Poland (NCN) grant HARMONIA 10 no. 2018/30/M/ST2/00799.
- We gratefully acknowledge Poland's high-performance computing infrastructure PLGrid (HPC Centers: ACK Cyfronet AGH) for providing computer facilities and support within computational grant no. PLG/2022/015994.
- This work was funded in part by the Swiss National Science Foundation.
- This work has been carried out within the framework of the EUROfusion Consortium, funded by the European Union via the Euratom Research and Training Programme (Grant Agreement No 101052200 — EUROfusion). Views and opinions expressed are however those of the author(s) only and do not necessarily reflect those of the European Union or the European Commission. Neither the European Union nor the European Commission can be held responsible for them.
- This work has been published in the framework of the international project co-financed by the Polish Ministry of Education and Science, as program "PMW", contracts 5235/HEU - EURATOM/2022/2 and 5253/HEU-EURATOM/2022/2.



Backup slides



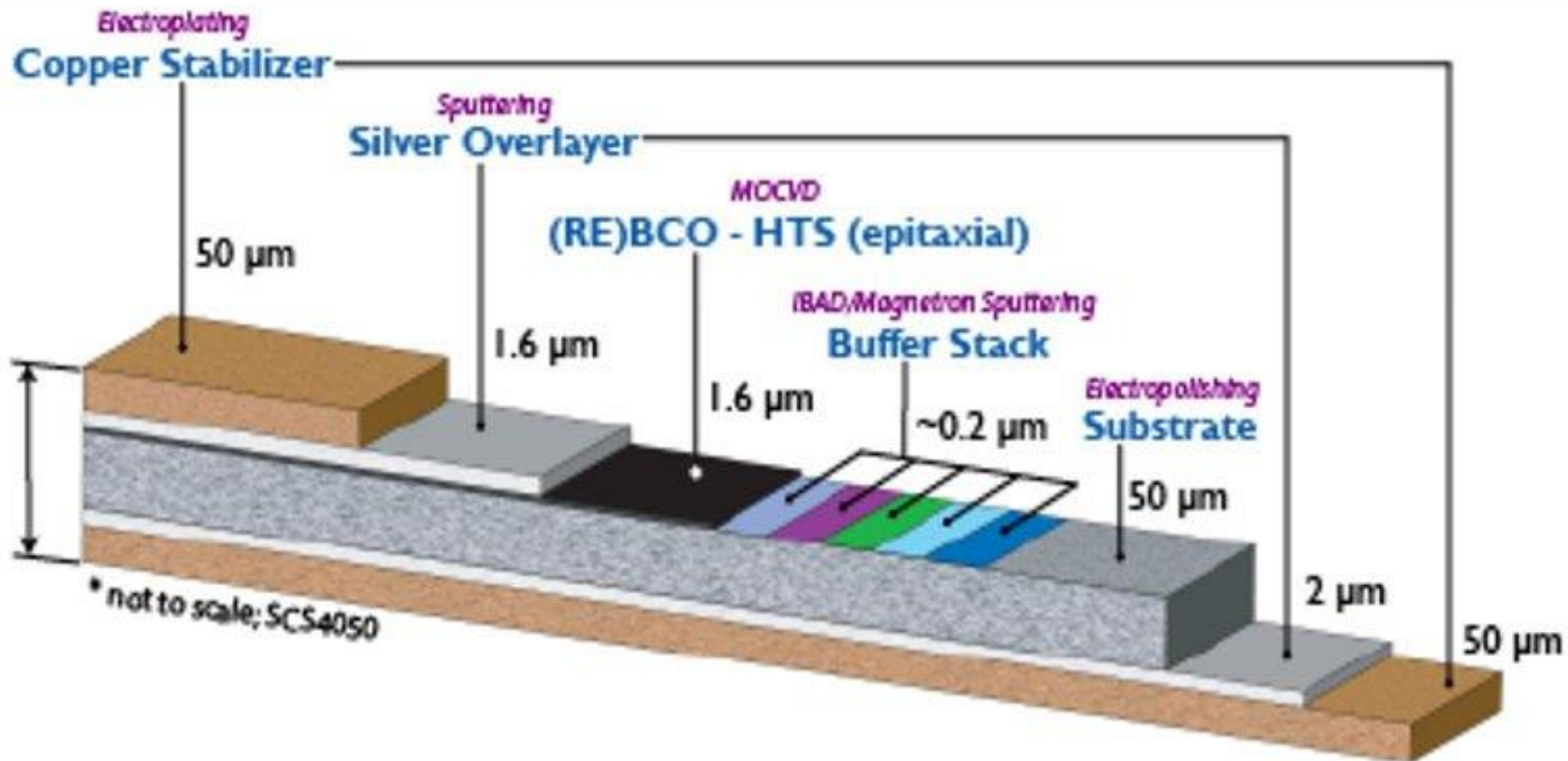




THE HENRYK NIEWODNICZAŃSKI
INSTITUTE OF NUCLEAR PHYSICS
POLISH ACADEMY OF SCIENCES



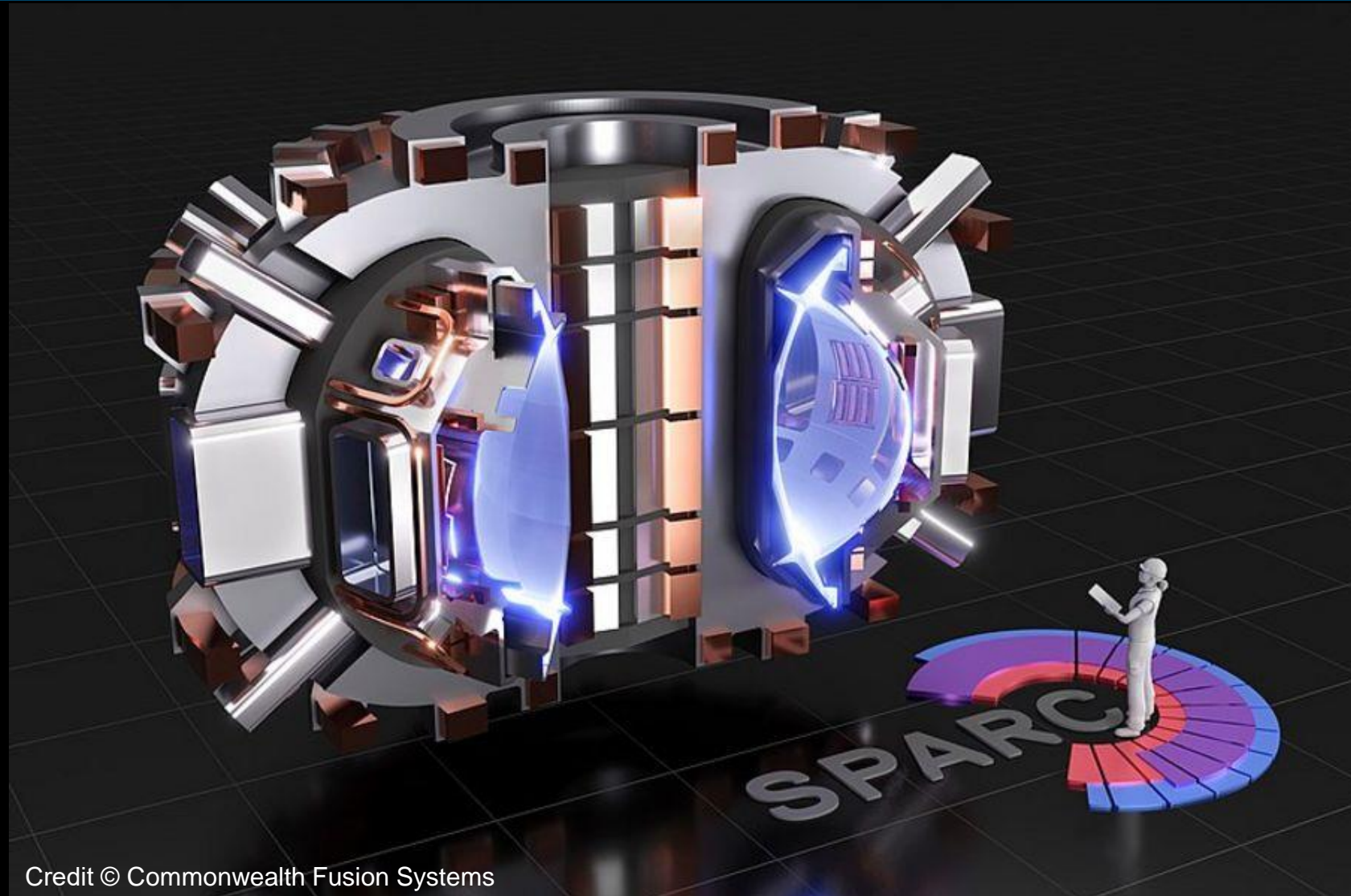
Credit © UKAES



Credit © Commonwealth Fusion Systems



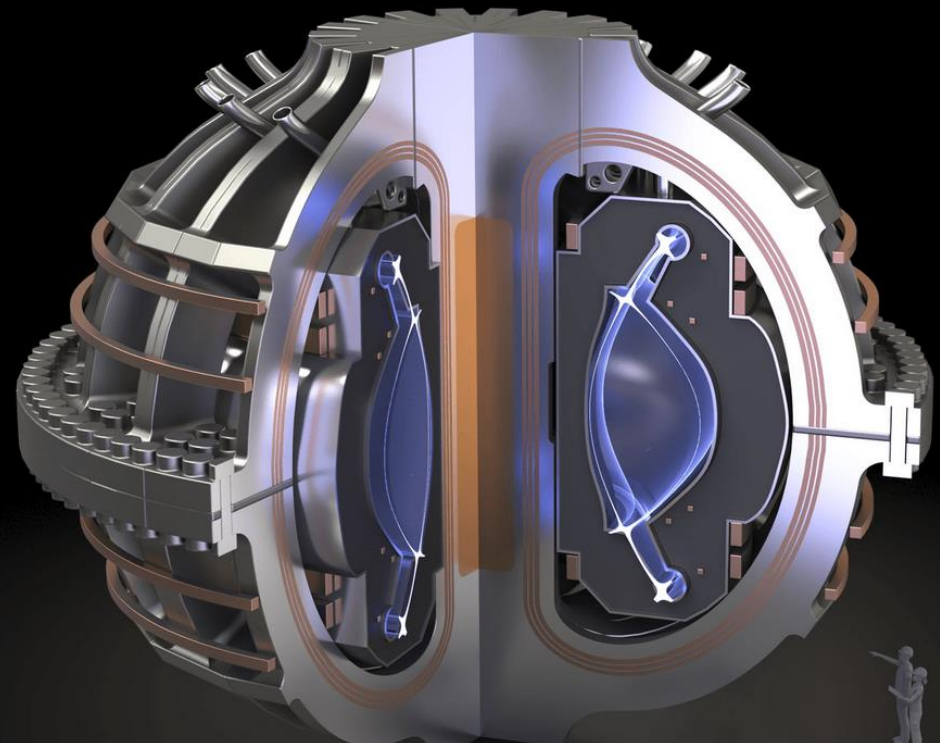
THE HENRYK NIEWODNICZAŃSKI
INSTITUTE OF NUCLEAR PHYSICS
POLISH ACADEMY OF SCIENCES



Credit © Commonwealth Fusion Systems

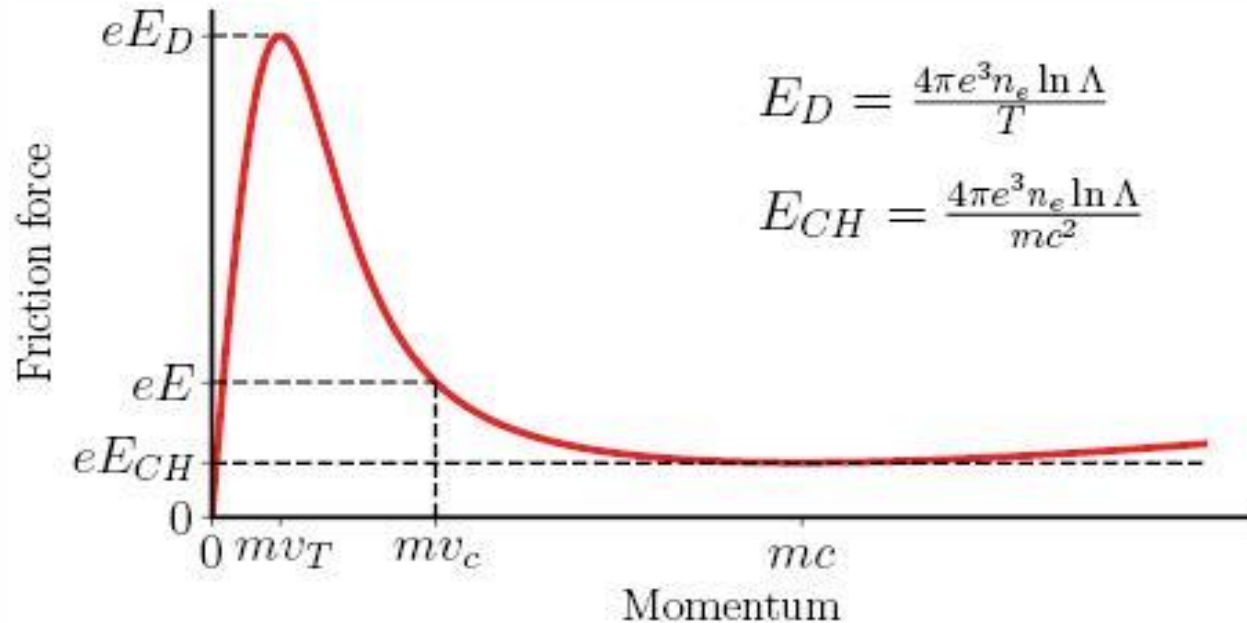


THE HENRYK NIEWODNICZAŃSKI
INSTITUTE OF NUCLEAR PHYSICS
POLISH ACADEMY OF SCIENCES



Credit © Commonwealth Fusion Systems

Friction force



Multi-exponential PT model - PT_opt

	Grouping of the electrons in the PT _{opt} model				
Electron group	N_1	N_2	N_3	N_4	N_5
Max. number of bound electrons in each group	2	8	18	28	rest
Total bound electrons when group fully occupied	2	10	28	54	rest

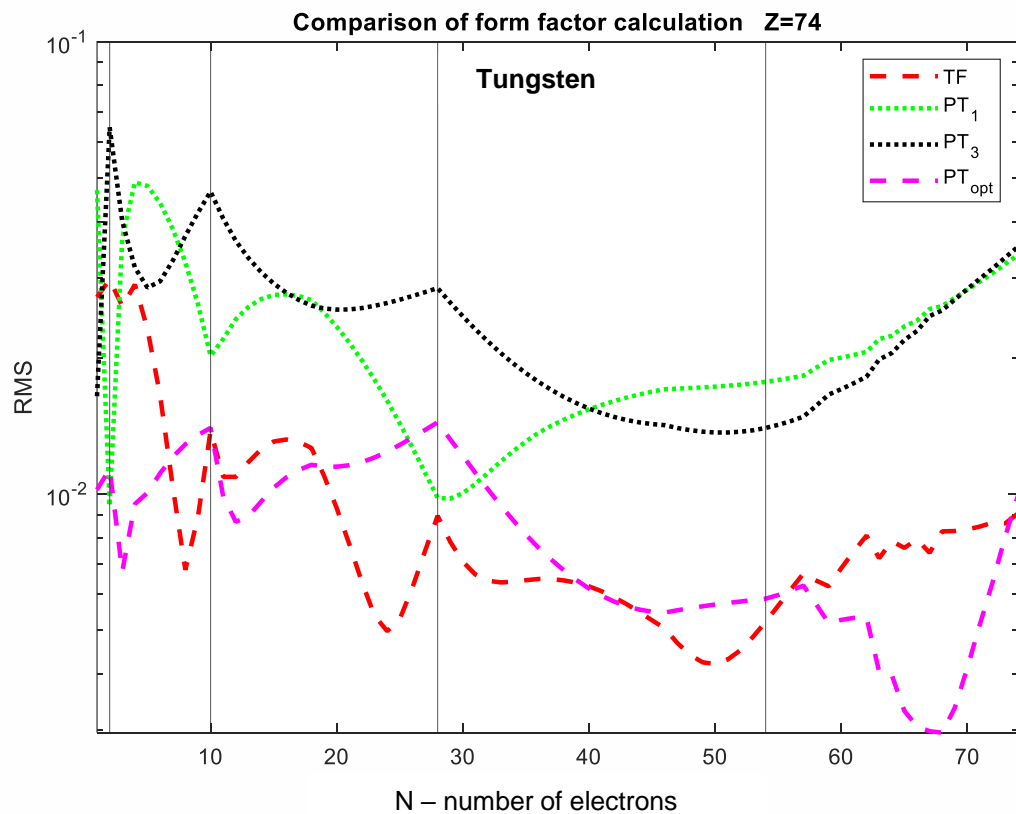
$$a_i(Z, N) = 1 / \sqrt{\lambda_i^2 * \frac{(1-x^{n_{s,i}+1})}{1-x}}, \text{ where } x = \frac{Z-N}{Z}$$

$$\lambda_i(Z) = c_{1,i} * Z^{c_{2,i}}$$

$$n_{s,i}(Z) = c_{3,i} * Z^{c_{4,i}}$$

		Optimized parameters for PT _{opt} model				
		i = 1	i = 2	i = 3	i = 4	i = 5
$\lambda_i(Z)$	$c_{1,i}$	1.1831	0.1738	0.0913	0.0182	0.7702
	$c_{2,i}$	0.8368	1.0987	0.9642	1.2535	0.2618
$n_{s,i}(Z)$	$c_{3,i}$	0.3841	0.6170	1.0000	1.0000	1.0000
	$c_{4,i}$	0.5883	0.0461	1.0000	1.0000	1.0000

Results: PT_opt

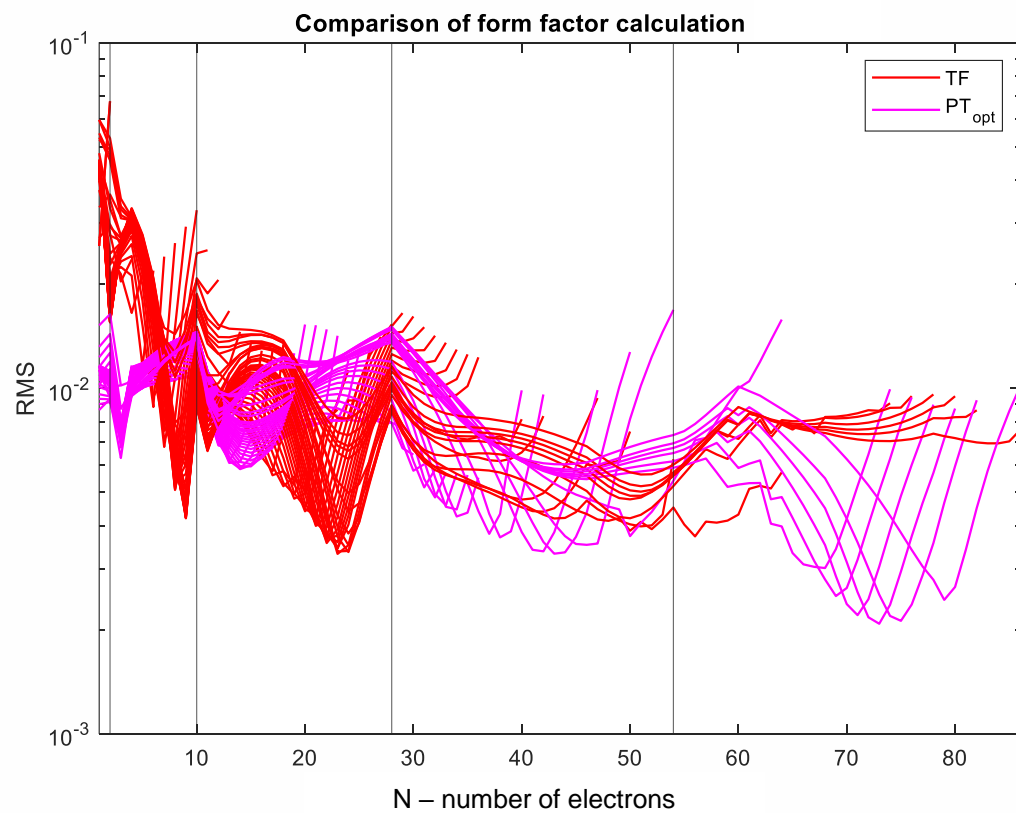


DESCRIPTION

- RMS of the **absolute** difference between form factors calculated with DFT and TF/TP electron density models:

$$\sqrt{\frac{1}{N^2} * \frac{1}{n} * \sum_{i=1}^n (F_{DFT}(q_i) - F_2(q_i))^2}$$

Results: Comparison of PT_opt model to TF model



DESCRIPTION

- Each line on the plot represents results for one element



- DREAM (Disruption and Runaway Electron Analysis Model) code
- Fully-implicitly solver: evolution of temperature, density, current density and electric field, electron distribution function.
- Drift-kinetic model with a fully relativistic Fokker-Planck test-particle operator for electron-electron collisions, synchrotron radiation reaction force, an avalanche operator, bremsstrahlung and screening effects in a partially ionised plasma
- Parts of the electron phase space modelled kinetically, and the remainder described by fluid equations.
- In the presented work a fully fluid representation of plasma was compared with a reduced kinetic model



Inelastic collisions – Bethe formula

$$\frac{dE}{dx} = 4\pi r_e^2 m_e^2 c^2 \frac{1}{\beta^2} \frac{N_A Z \rho}{A} \int_{b_{min}}^{b_{max}} \frac{db}{b}$$

$$\frac{db}{b} = -\frac{1}{2} \frac{dE}{E}$$

$$\frac{dE}{dx} = -2\pi r_e^2 m_e^2 c^2 \frac{1}{\beta^2} \frac{N_A Z \rho}{A} \int_{E_{min}}^{E_{max}} \frac{dE}{E}$$

$$\int_{E_{min}}^{E_{max}} \frac{dE}{E} = \ln\left(\frac{E_{max}}{E_{min}}\right)$$



Inelastic collisions – Stopping power

- One potential problem arising from the use of Bethe theory is that this model is valid for $2mv^2 \gg I$, otherwise the \ln term will approach 0.
- In case of Tungsten, ions can reach I as high as 100 keV (for Hydrogen like atoms it follows the Z^2 dependence)
- In tokamak plasma, expected I is 3 – 13 keV, and lower bound of fast electrons from LHCD is 20 keV
- In LUKE approximated formula is used, to avoid numerical problems



Inelastic collisions – Stopping power

$$\nu_s^{ee} = 4\pi c r_0^2 \frac{\gamma}{p^3} [n_e \ln \Lambda^{ee} + n_i N (\ln h - \beta^2)]$$

where n_e – density of free electrons in plasma, n_i – density of ions in plasma, $\beta = v/c$, $h = \sqrt{\gamma - 1}(mc^2/I)$, γ – Lorentz factor, I – mean excitation energy, N – number of bound electrons in the ion

$$\ln \Lambda^{ee} = \ln \Lambda + 1/k \ln \left(1 + [2(\gamma - 1)/p_{Te}^2]^{k/2} \right),$$

where p_{Te} – thermal momentum, k - model parameter.



Inelastic collisions - Mean excitation energy

- In [Sauer 2020] it is mentioned, that result for ions of elements with Z 20-30 so far have only been reported for neutral atoms using Hartree-Slater wavefunctions and the LPA
- Results from Sauer et.al. contains only non-relativistic calculations
- They state accuracy of the basis sets as a crucial factor for successful calculation of the mean excitation energy



Inelastic collisions - Mean excitation energy

- Also in papers from Sauer et.al it is mentioned, that for the hydrogen like atoms:

$$I_0(Z) = I_0(H)Z^2$$

Which can be generalized for the K shell to the

$$I_0(Z) = I_0(H)Z_{eff}^2$$

Where $Z_{eff} = Z - S$, where S is screening constant equal 0 for H like ions and 0.3 for He like atoms (similar as in Slater original proposition for screening constants)

Unfortunately, this only works with the K shell electrons

Local Plasma Approximation

- Lindhard model is based on the TF atomic model, which is not accurate for innermost electrons
- The γ constant is derived from the analysis of the effective frequency as:

$$\omega_{eff} = \sqrt{\omega_0^2 + \omega_r^2}$$

Where $\omega_r \approx \omega_0$, and thus:

$$\omega_{eff} = \sqrt{\omega_0^2 + \omega_r^2} = \sqrt{\omega_0^2 + \omega_0^2} = \sqrt{2}\omega_0$$

ω_0 is the classical resonance frequency of the electron gas

ω_r is derived from the revolution frequency of the independent particle model

- It is stated, that for light elements where polarization is of minor importance, the γ will approach 1

Source: J. Lindhard and M. Scharff, K. Dan. Vidensk. Selsk. Mat. Fys. Medd. 27 (1953) no. 15.

Results – gamma fitting

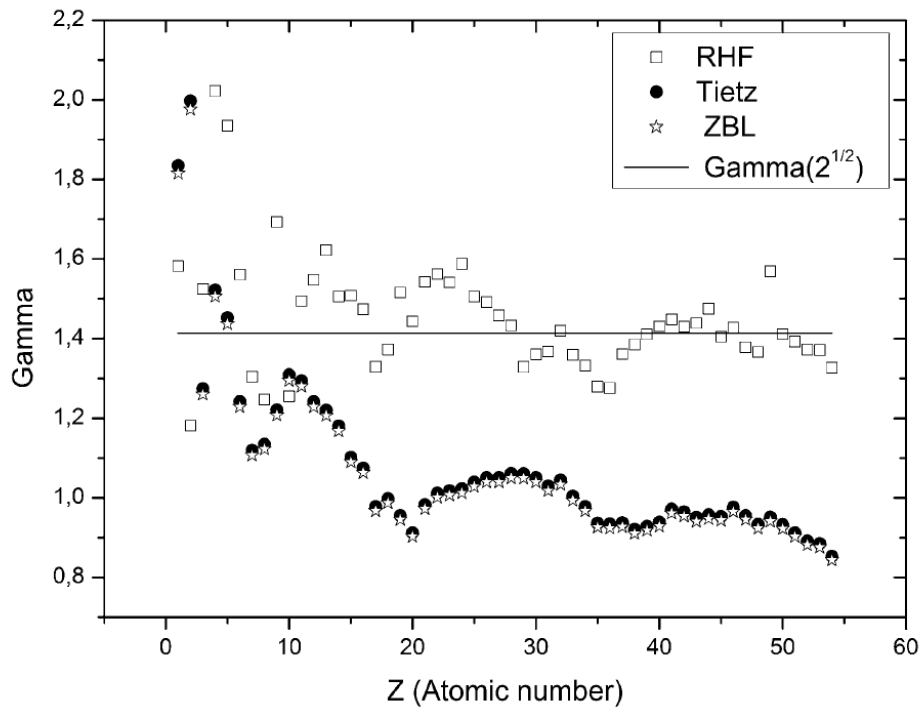
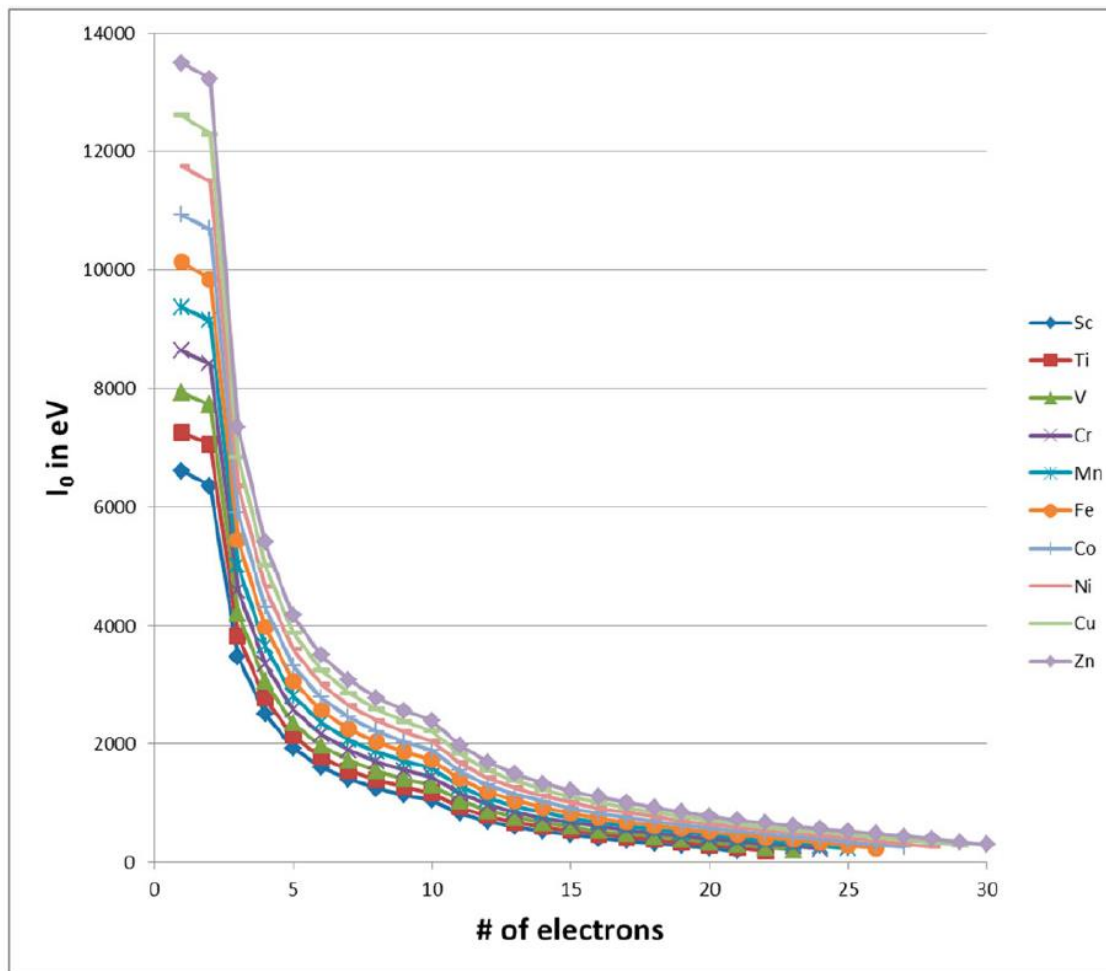


Fig. 2 Gamma values for $Z \leq 54$

Source: M. Tufan and Z. Yüksel, Indian Journal of Physics v. 93, p. 301–305 (2019)

DESCRIPTION

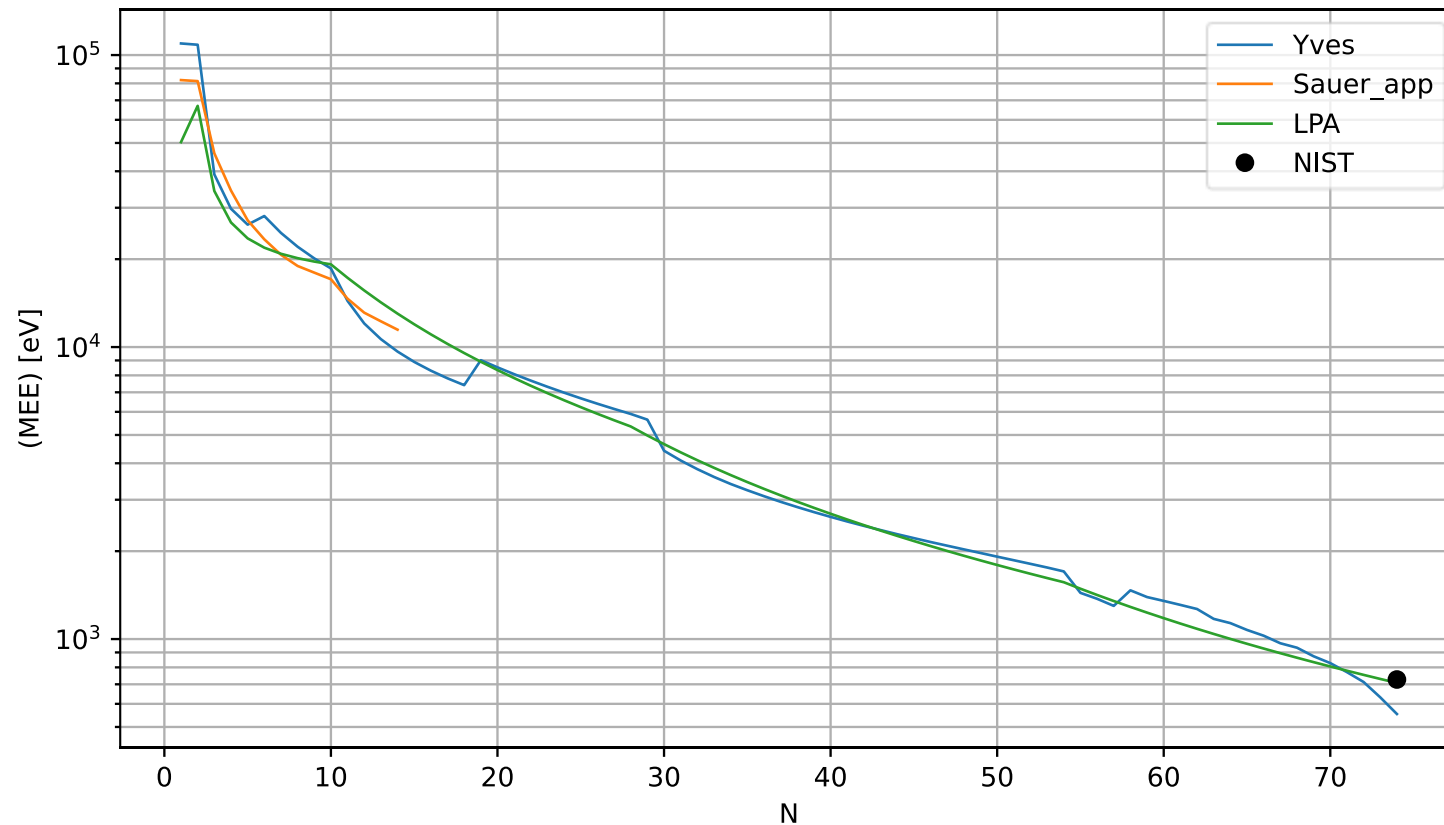
- The modified γ values was varying from 0.8 to 2
- RHF (Roothan-Hartree-Fock) - the γ oscillates around 1.4 as expected
- Tietz and ZBL – TF with different solutions of the TF function



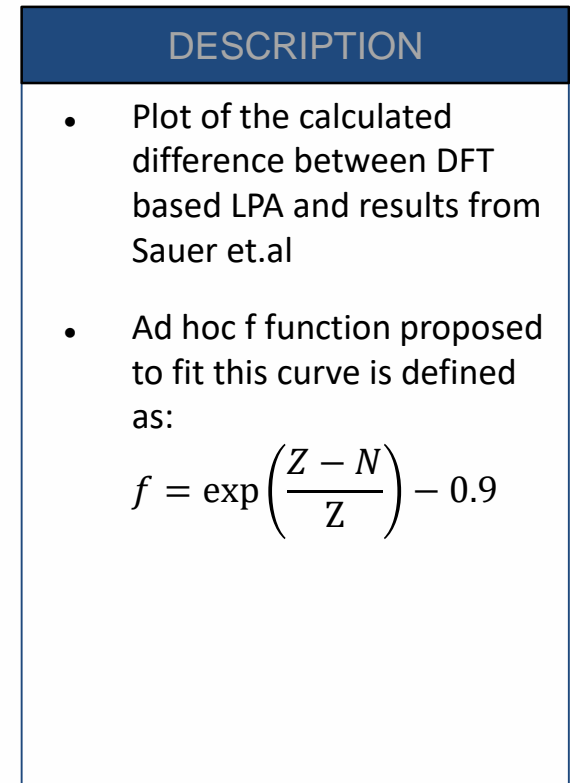
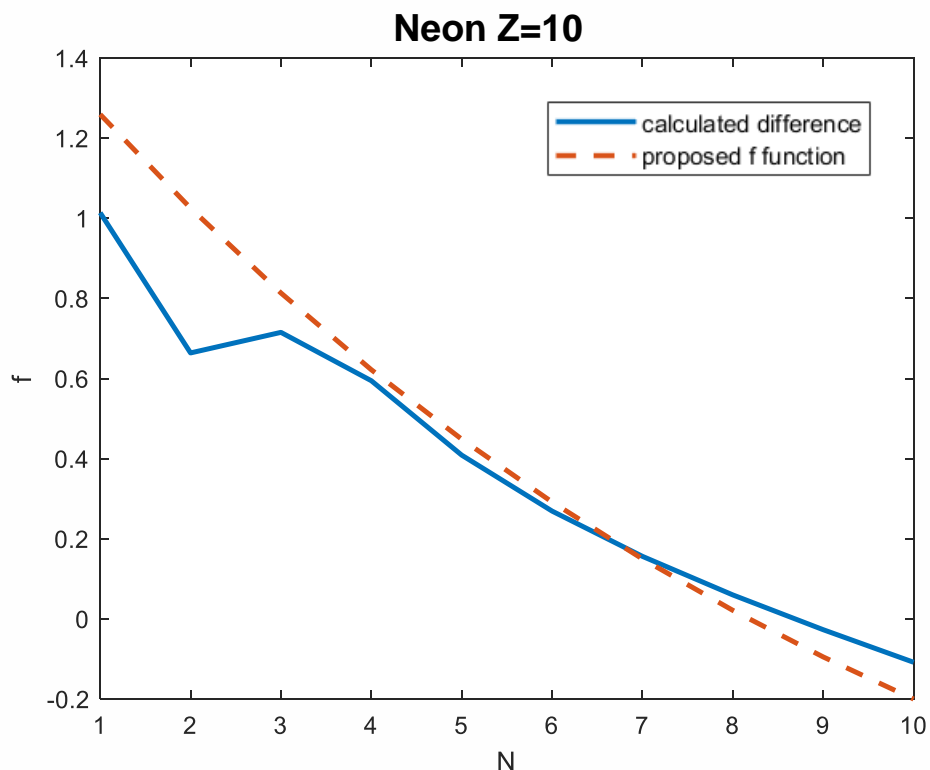
The mean excitation energies of the 3d elements and their cations as function of the number of electrons.

Source: [Sauer 2020]

Mean Excitation Energy - Tungsten

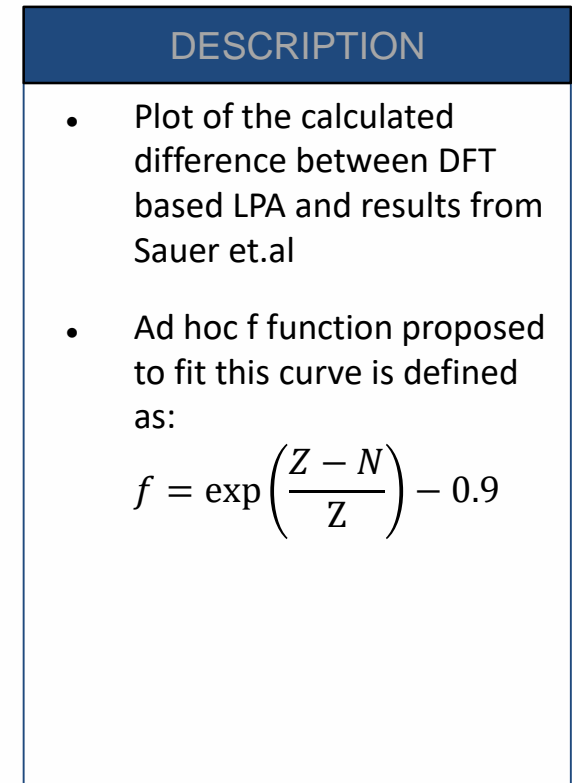
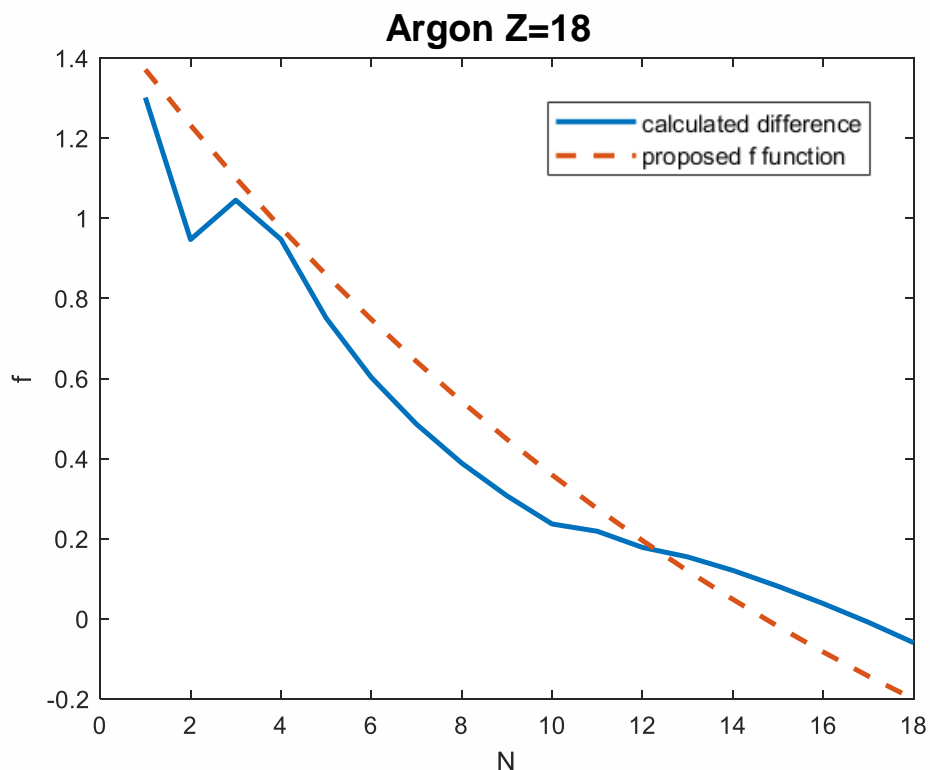


Results – f calculation



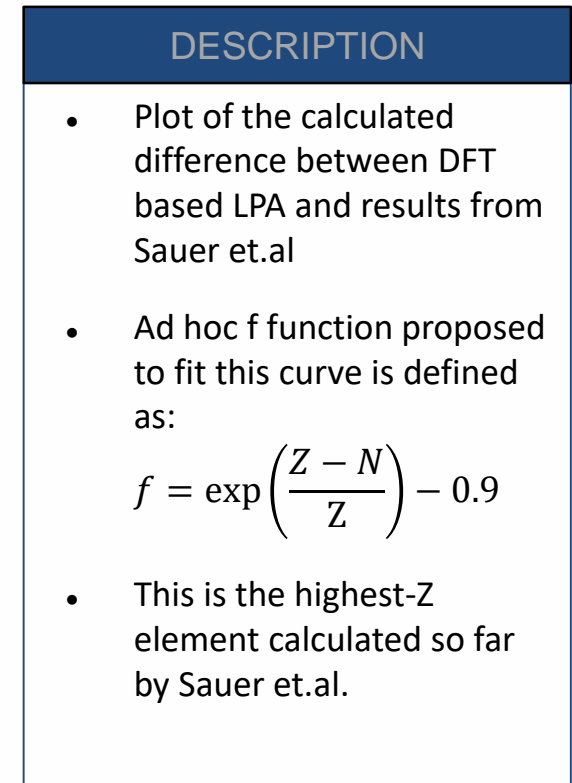
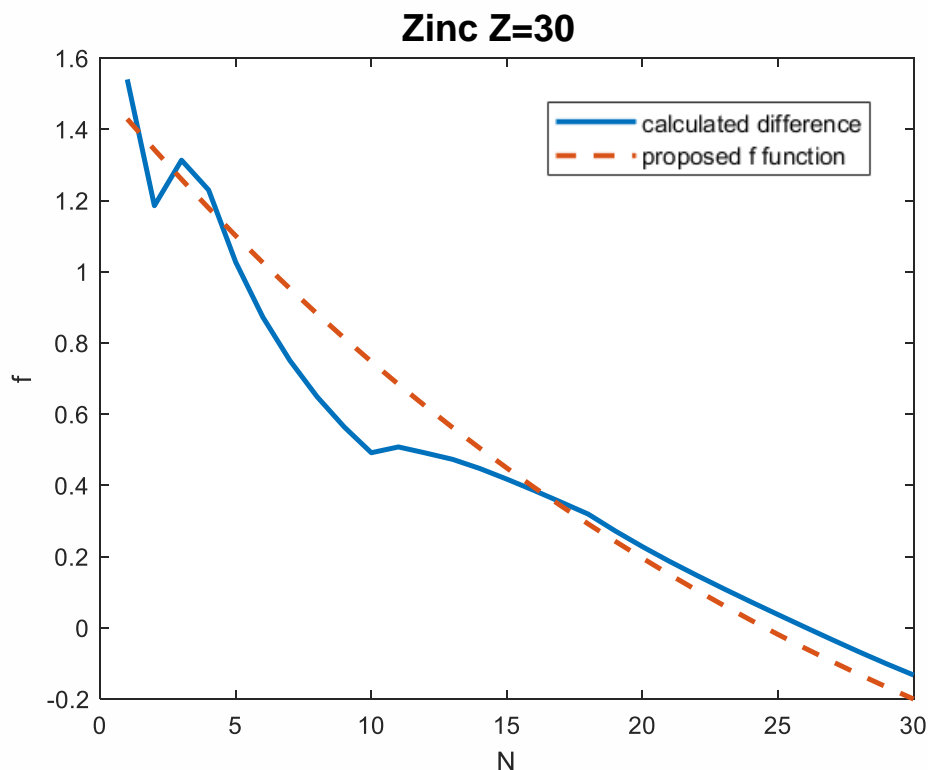
Source: [Sauer 2015]

Results – f calculation



Source: [Sauer 2015]

Results – f calculation



Source: [Sauer 2020]

Simulation setup

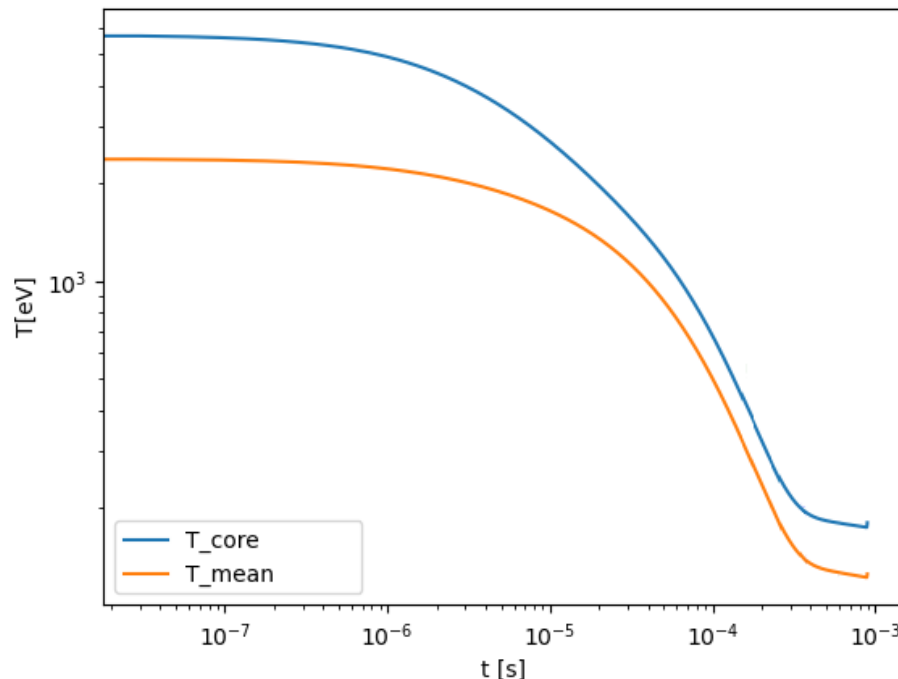
Parameter	ASDEX-like [Hoppe 2021]	ITER-like [Pusztai 2022]
Major radius R_m	1.65 m	6.0 m
Minor radius a	0.5 m	2.0 m
Wall radius b	0.55 m	2.833 m
Elongation at edge $\kappa(a)$	1.15	1.82
Toroidal magnetic field B_0	2.5 T	5.3 T
Initial plasma current $I_{p,0}$	800 kA	15 MA
Resistive wall time	10 ms	500 ms

Source: J. Walkowiak et al 2024 *Nucl. Fusion* 64 036024
M. Hoppe et al, 2021, *Comput. Phys. Commun.* 268 108098
I. Pusztai, 2022, *Journal of Plasma Physics*, 88, 4, 905880409

Thermal Quench (TQ) time

In general, the TQ shape is different than in the case of the lighter impurities, as tungsten radiates at all temperatures.

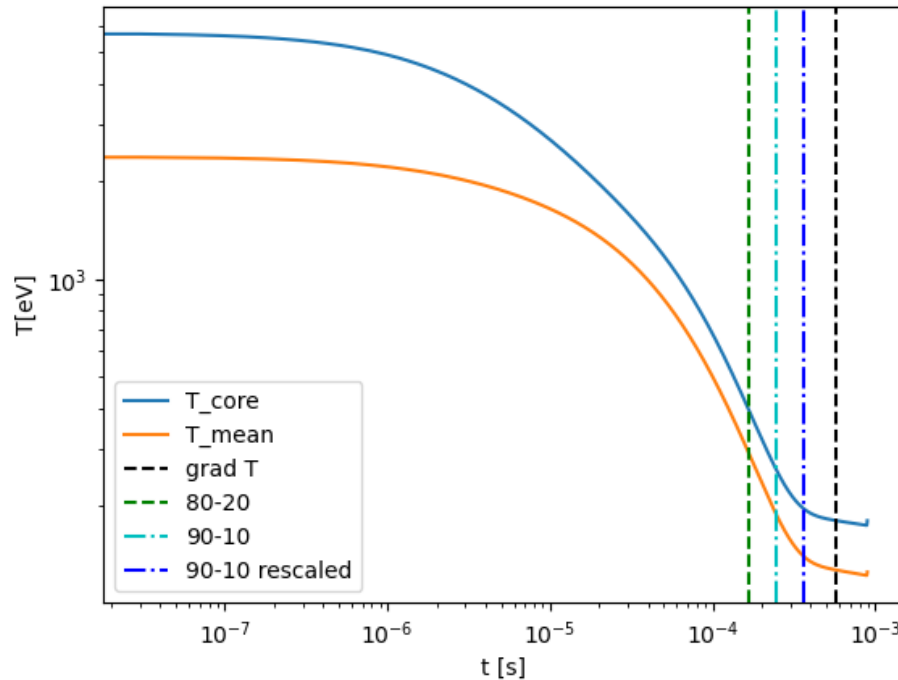
Time evolution of the core and mean temperature



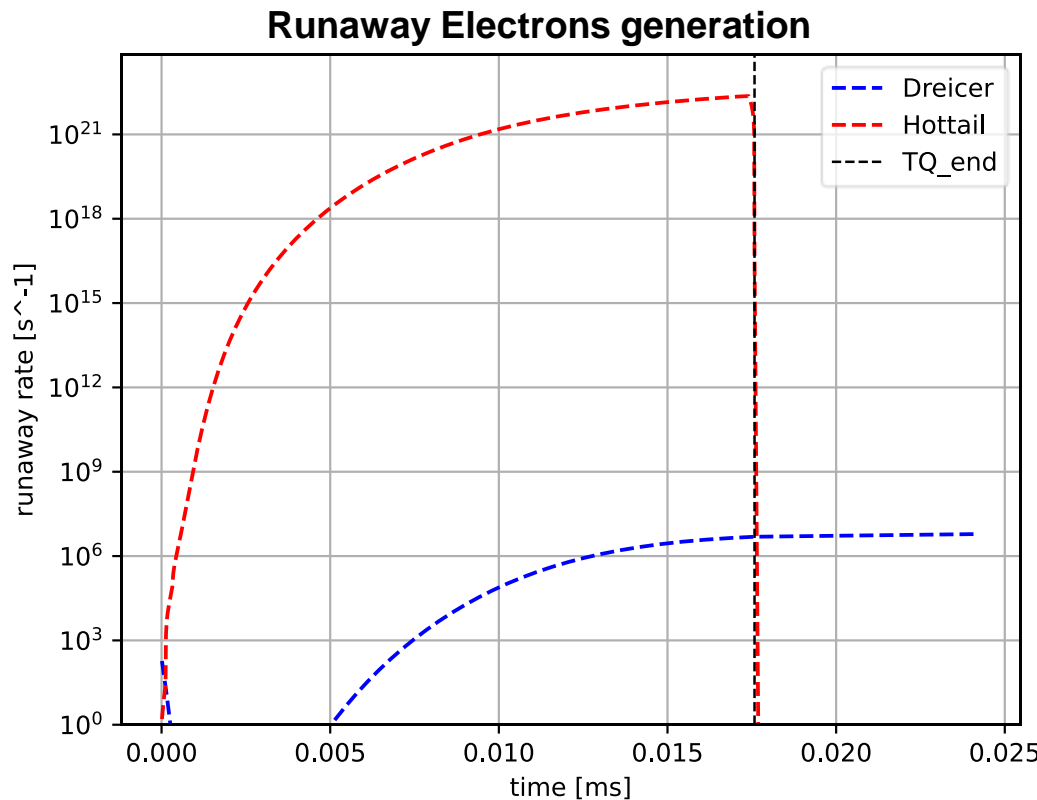
Thermal Quench (TQ) time

In general, the TQ shape is different than in the case of the lighter impurities, as tungsten radiates at all temperatures.

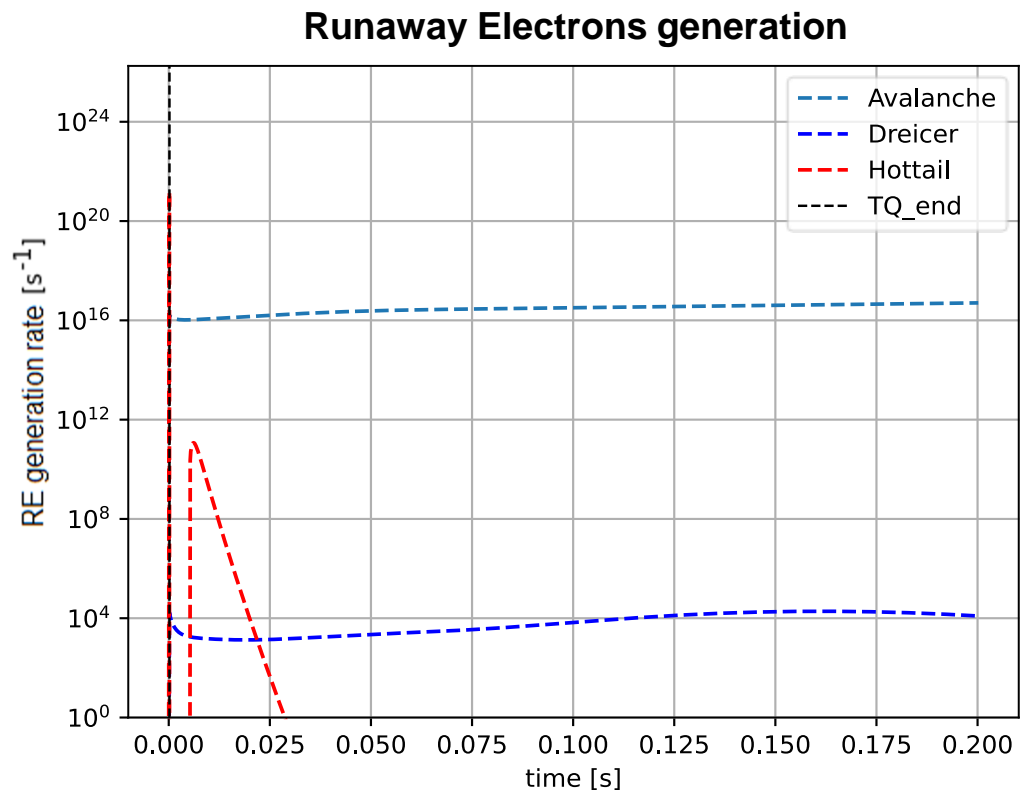
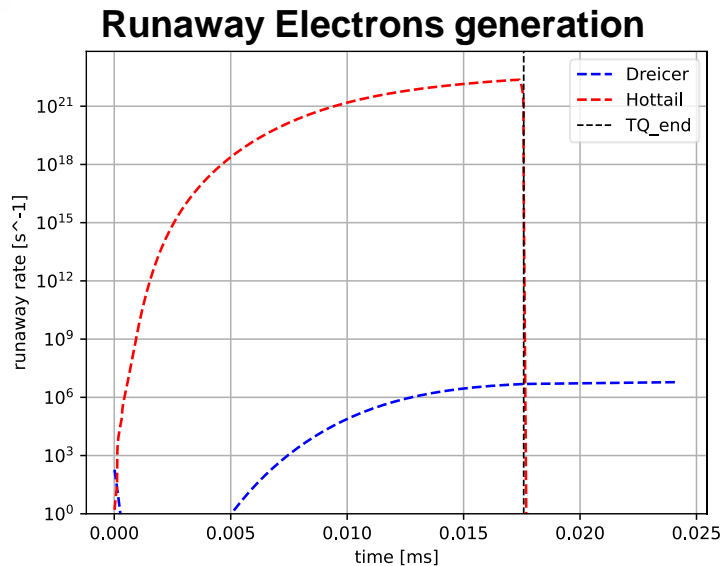
Time evolution of the core and mean temperature



Runaway electrons (RE) generation: Dreicer, hottail and avalanche



Runaway electrons (RE) generation: Dreicer, hottail and avalanche



Runaway electrons (RE) generation: Dreicer, hottail and avalanche

